



***Unveiling the Massive Black Hole
cosmic history with eLISA/NGO***

Alberto Sesana

Albert Einstein Institute, Golm

Bologna 08/03/2012

OUTLINE

- 1- Gravitational wave generation and detection:
how does it work?**
- 2- Waveform modelling and parameter estimation.**
- 3- Why do we care? The hierarchical model: MBH
assembly and growth**
- 4- Probing the MBH evolution with eLISA/NGO**

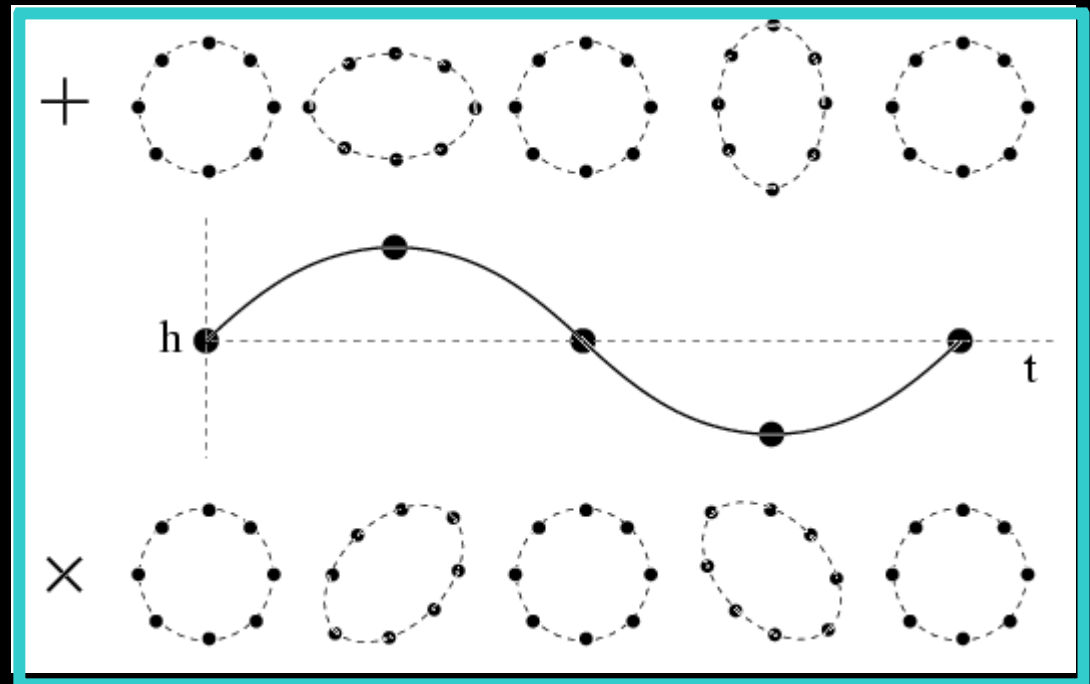
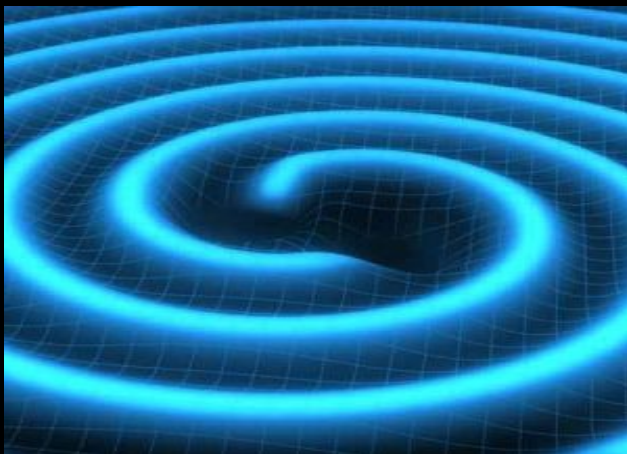
Directly from general relativity

Every accelerating mass distribution with non-zero quadrupole momentum emits GWs!

$$g_{\mu\nu} = \eta_{\mu\nu} + h_{\mu\nu}, \quad h_{\mu\nu} \ll 1$$

Perturbed Minkowski metric tensor

$$g_{\mu\nu} = \begin{pmatrix} -1 & 0 & 0 & 0 \\ 0 & 1 & 0 & 0 \\ 0 & 0 & 1 + h_+^{TT} & h_\times^{TT} \\ 0 & 0 & h_\times^{TT} & 1 - h_+^{TT} \end{pmatrix}$$

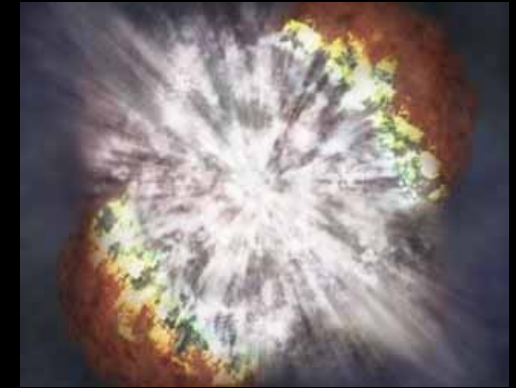


Perturbation perpendicular to the wave propagation direction

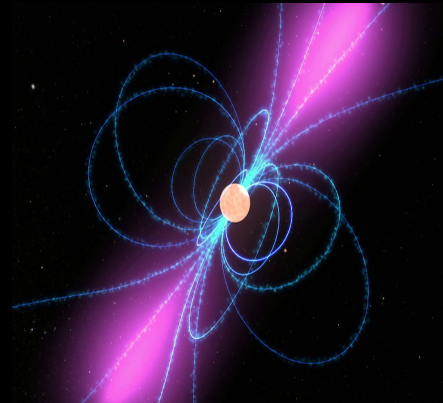
Gravitational wave sources

Massive compact systems with a time varying mass quadrupole momentum:

1-collapses and explosions (supernovae, GRBs)

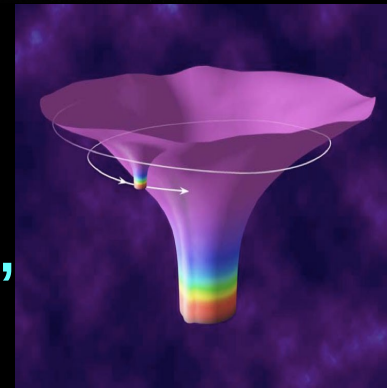


2-rotating asymmetric objects (pulsars, MSPs)

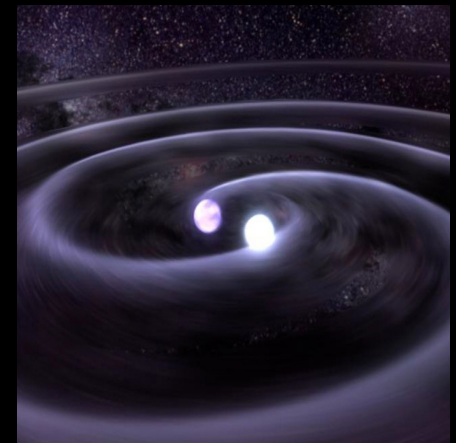


3-binary systems:

a-stellar compact remnants (WD-WD, NS-NS, NS-BH, BH-BH)



b-extreme mass ratio inspirals (EMRIs), CO falling into a massive black hole



c-massive black hole binaries (MBHBs) forming following galaxy mergers



Our main focus: binary systems

During the adiabatic inspiral, the compact objects can be approximated as point masses, and the evolution equations can be expanded in powers of $1/c$: *Post-Newtonian (PN) approximation*.

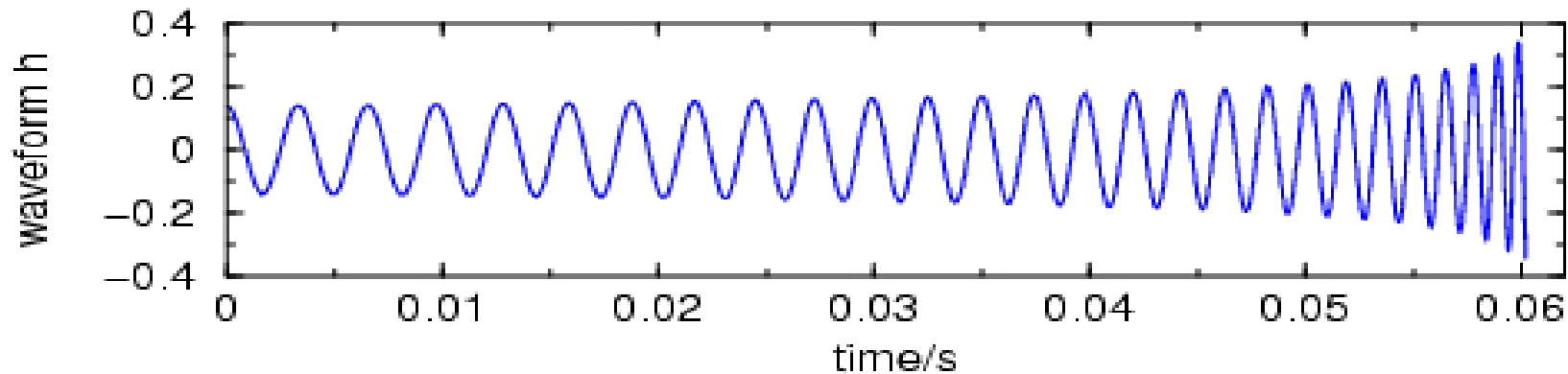
$$\frac{dv}{dt} = \frac{Gm}{r^2} \left\{ -\hat{\mathbf{n}} + \frac{1}{c^2} \mathbf{A}_{1\text{PN}} + \frac{1}{c^4} \mathbf{A}_{2\text{PN}} + \frac{1}{c^5} \mathbf{A}_{2.5\text{PN}} + \frac{1}{c^6} \mathbf{A}_{3\text{PN}} + \frac{1}{c^7} \mathbf{A}_{3.5\text{PN}} + \dots \right\},$$

$$h^{ij}(t, \mathbf{x}) = \frac{2Gm}{Rc^4} \left\{ Q^{ij} + \frac{1}{c} Q_{0.5\text{PN}}^{ij} + \frac{1}{c^2} Q_{1\text{PN}}^{ij} + \frac{1}{c^3} Q_{1.5\text{PN}}^{ij} + \frac{1}{c^4} Q_{2\text{PN}}^{ij} + \frac{1}{c^5} Q_{2.5\text{PN}}^{ij} + \dots \right\},$$

This way, we can build *gravitational waveforms for the inspiral*

Gravitational Wave of Compact Binary Inspiral

$m_1 = 1.75 \text{ Msun}$, $m_2 = 2.25 \text{ Msun}$, start $f = 150 \text{ Hz}$, coalescence: $f = 635 \text{ Hz}$



Our main focus: binary systems

During the adiabatic inspiral, the compact objects can be approximated as point masses, and the evolution equations can be expanded in powers of $1/c$: *Post-Newtonian (PN) approximation*.

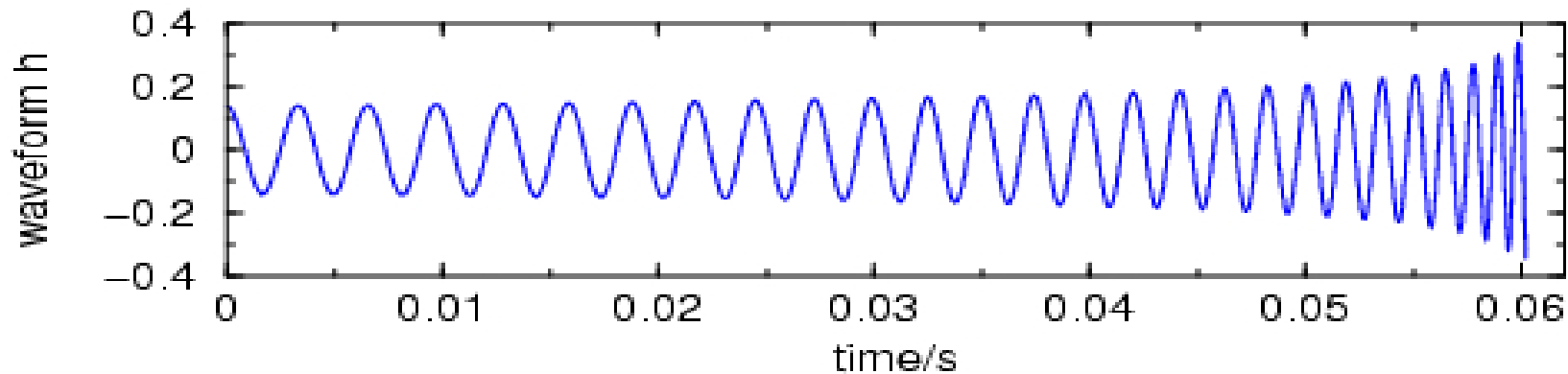
$$\frac{dv}{dt} = \frac{Gm}{r^2} \left\{ -\hat{\mathbf{n}} + \frac{1}{c^2} \mathbf{A}_{1\text{PN}} + \frac{1}{c^4} \mathbf{A}_{2\text{PN}} + \frac{1}{c^5} \mathbf{A}_{2.5\text{PN}} + \frac{1}{c^6} \mathbf{A}_{3\text{PN}} + \frac{1}{c^7} \mathbf{A}_{3.5\text{PN}} + \dots \right\},$$

$$h^{ij}(t, \mathbf{x}) = \frac{2Gm}{Rc^4} \left\{ Q^{ij} + \frac{1}{c} Q_{0.5\text{PN}}^{ij} + \frac{1}{c^2} Q_{1\text{PN}}^{ij} + \frac{1}{c^3} Q_{1.5\text{PN}}^{ij} + \frac{1}{c^4} Q_{2\text{PN}}^{ij} + \frac{1}{c^5} Q_{2.5\text{PN}}^{ij} + \dots \right\},$$

This way, we can build *gravitational waveforms for the inspiral*

Gravitational Wave of Compact Binary Inspiral

$m_1 = 1.75 \text{ Msun}$, $m_2 = 2.25 \text{ Msun}$, start $f = 150 \text{ Hz}$, coalescence: $f = 635 \text{ Hz}$

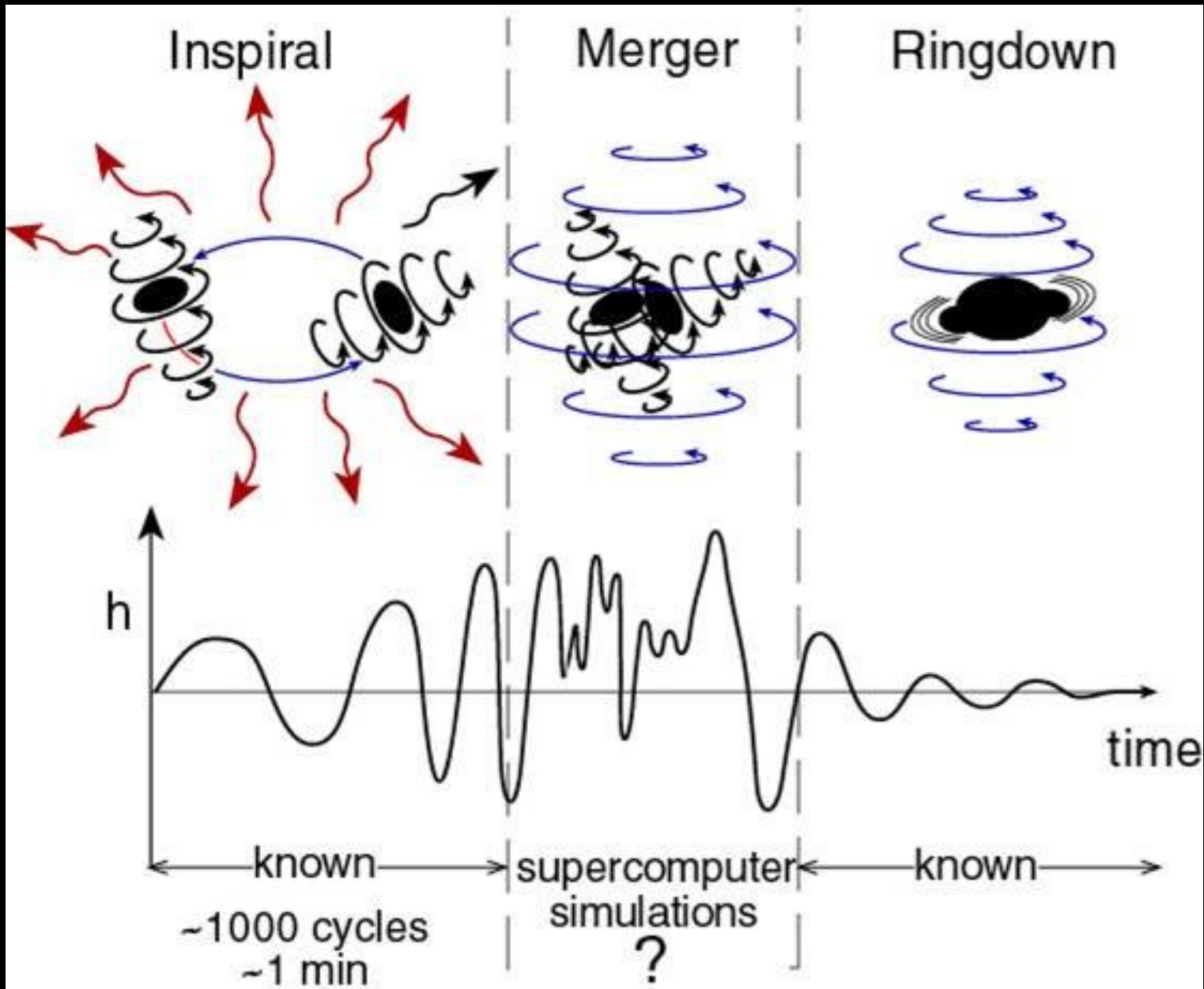


Warning!

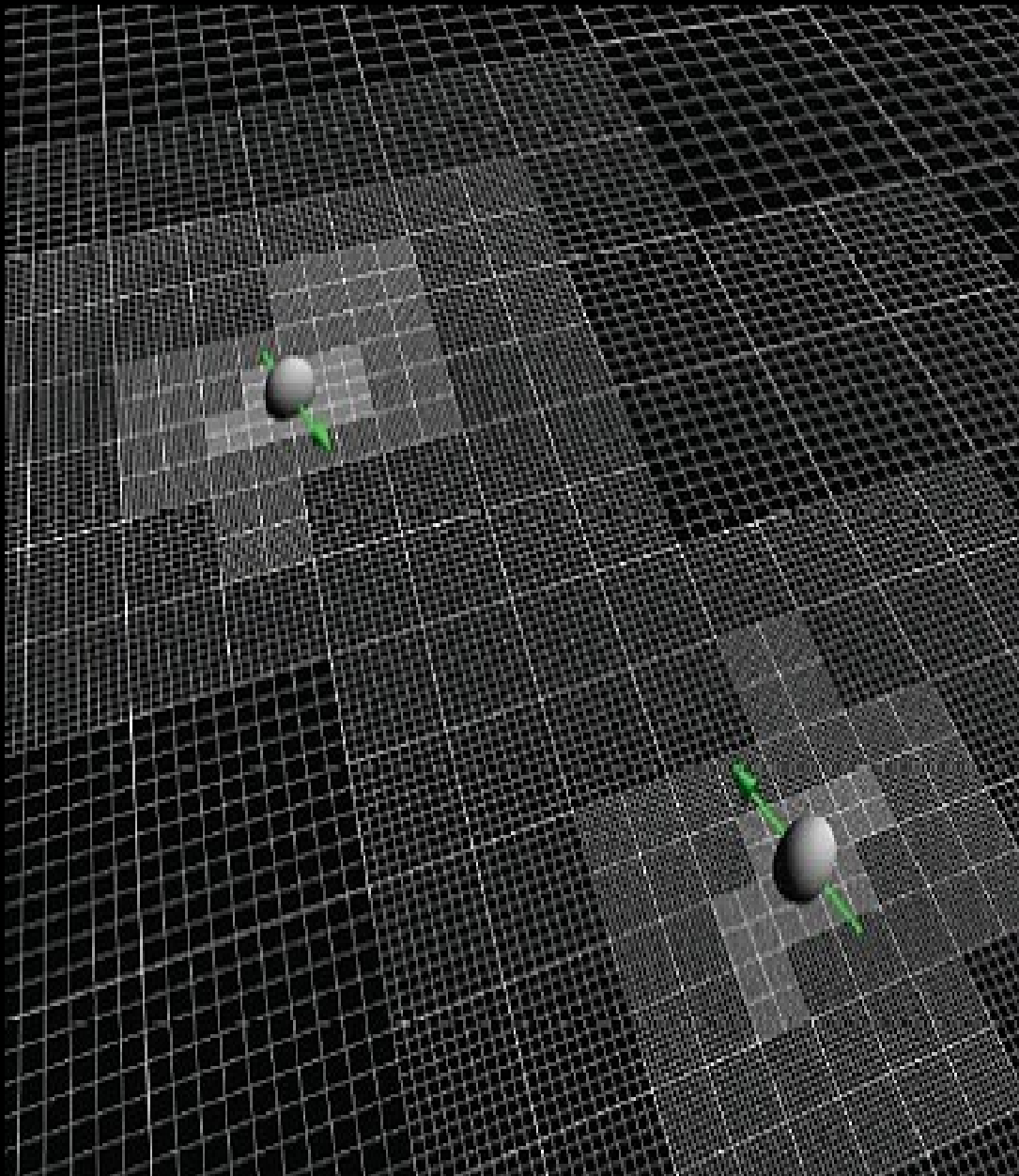
PN expansions are not unique. The resulting waveform slightly differ depending on the particular expansion employed and of the $1/c^n$ order of truncation (asymptotic series)

But what happens at the merger?

$v \sim c$, the PN approximation breaks down, and the evolution of the system is highly non linear



Credits: Kip Thorne

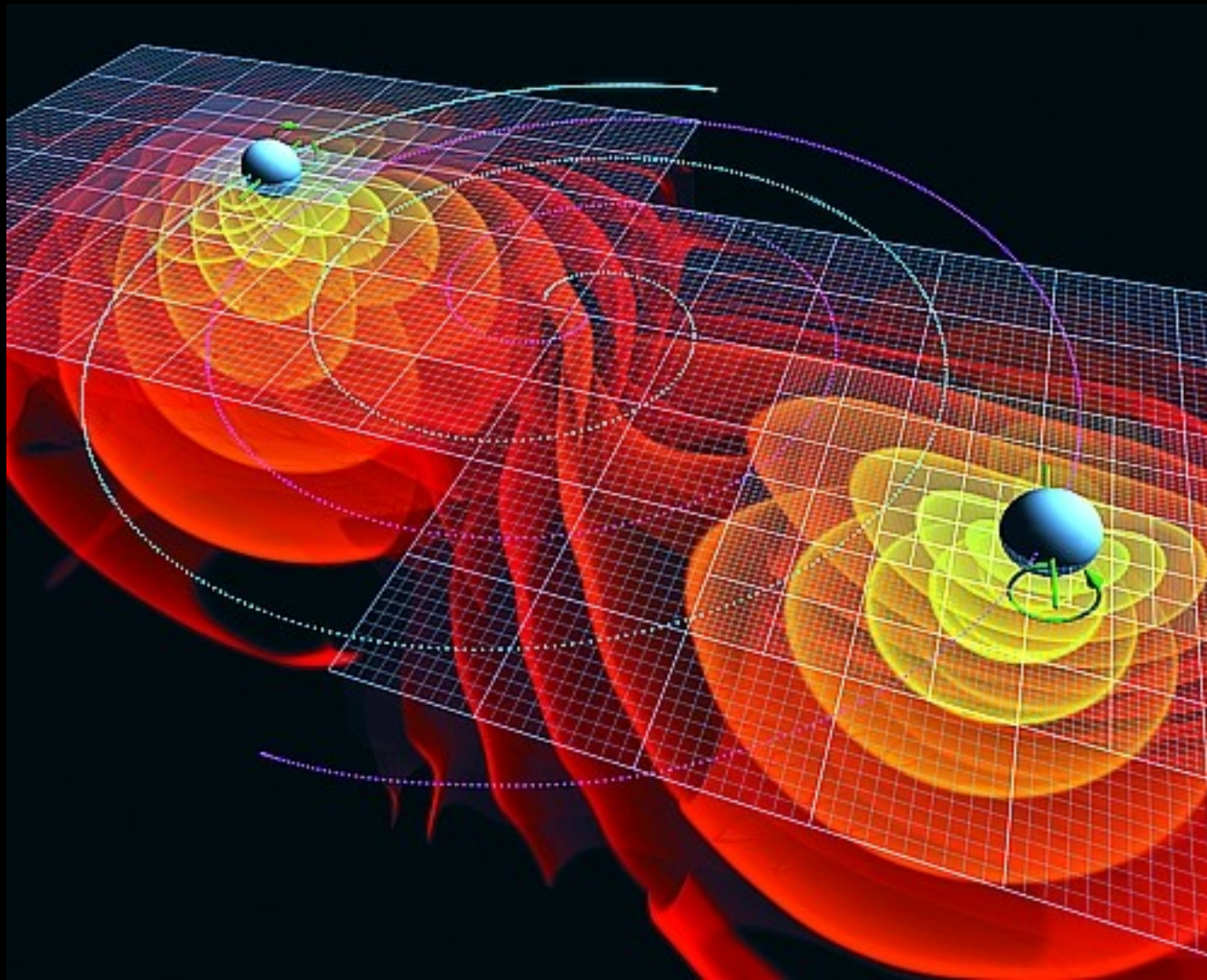


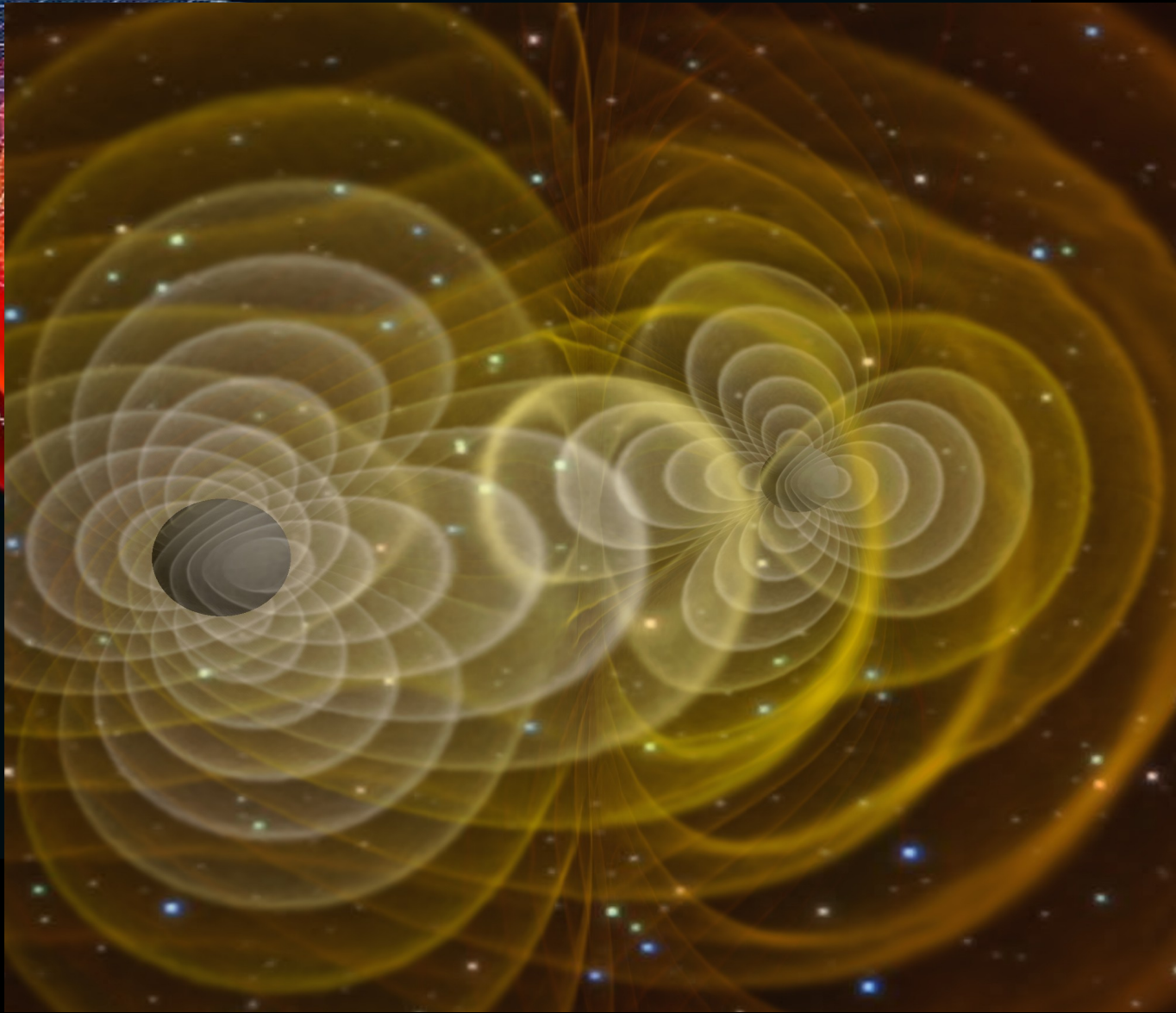
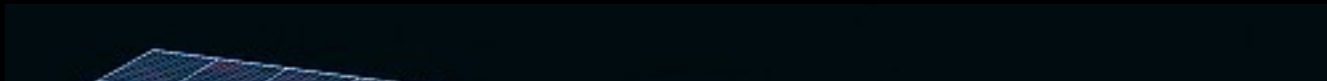
**2005: Numerical relativity
(NR) breakthrough!**
(Frans Pretorius)

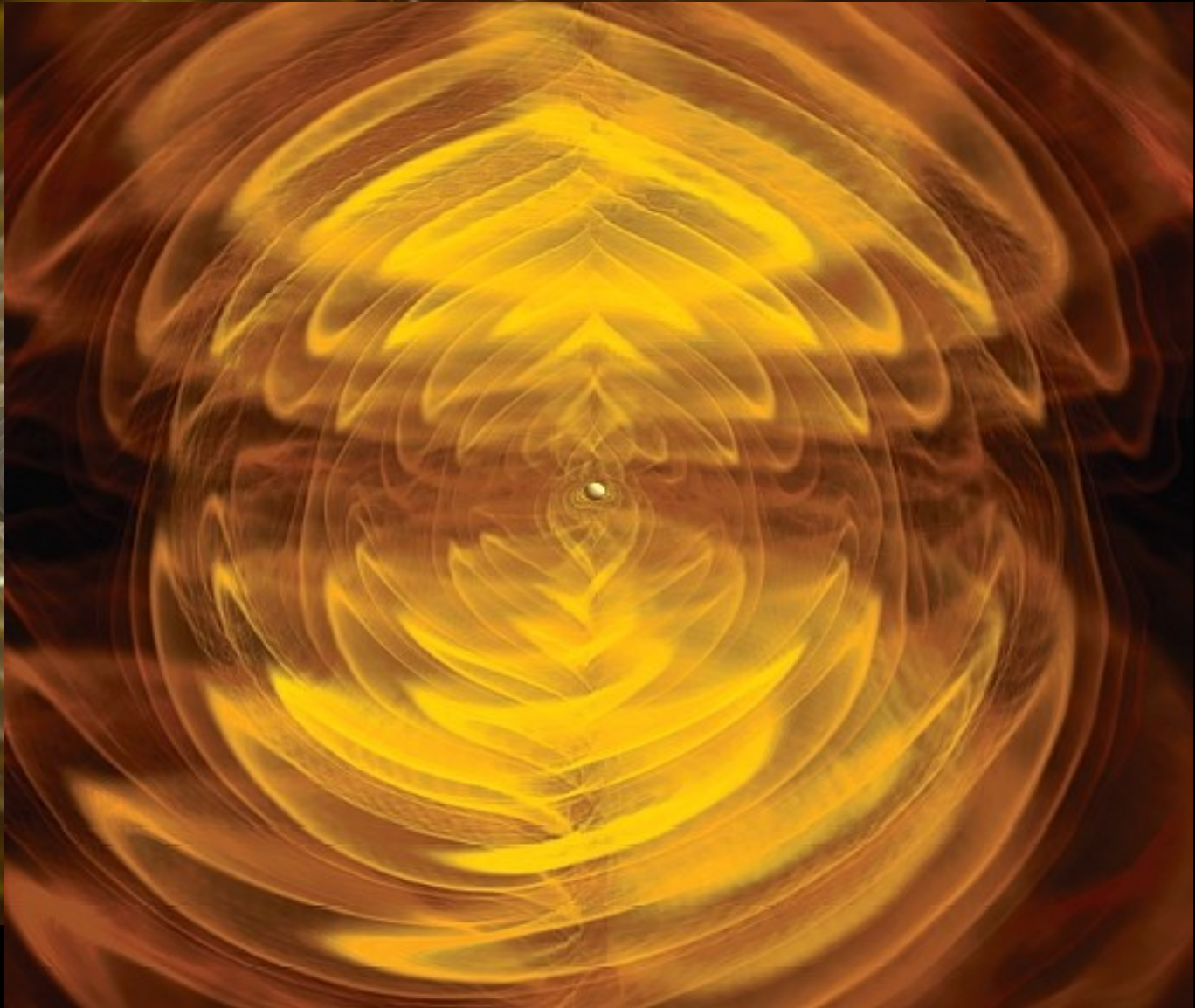
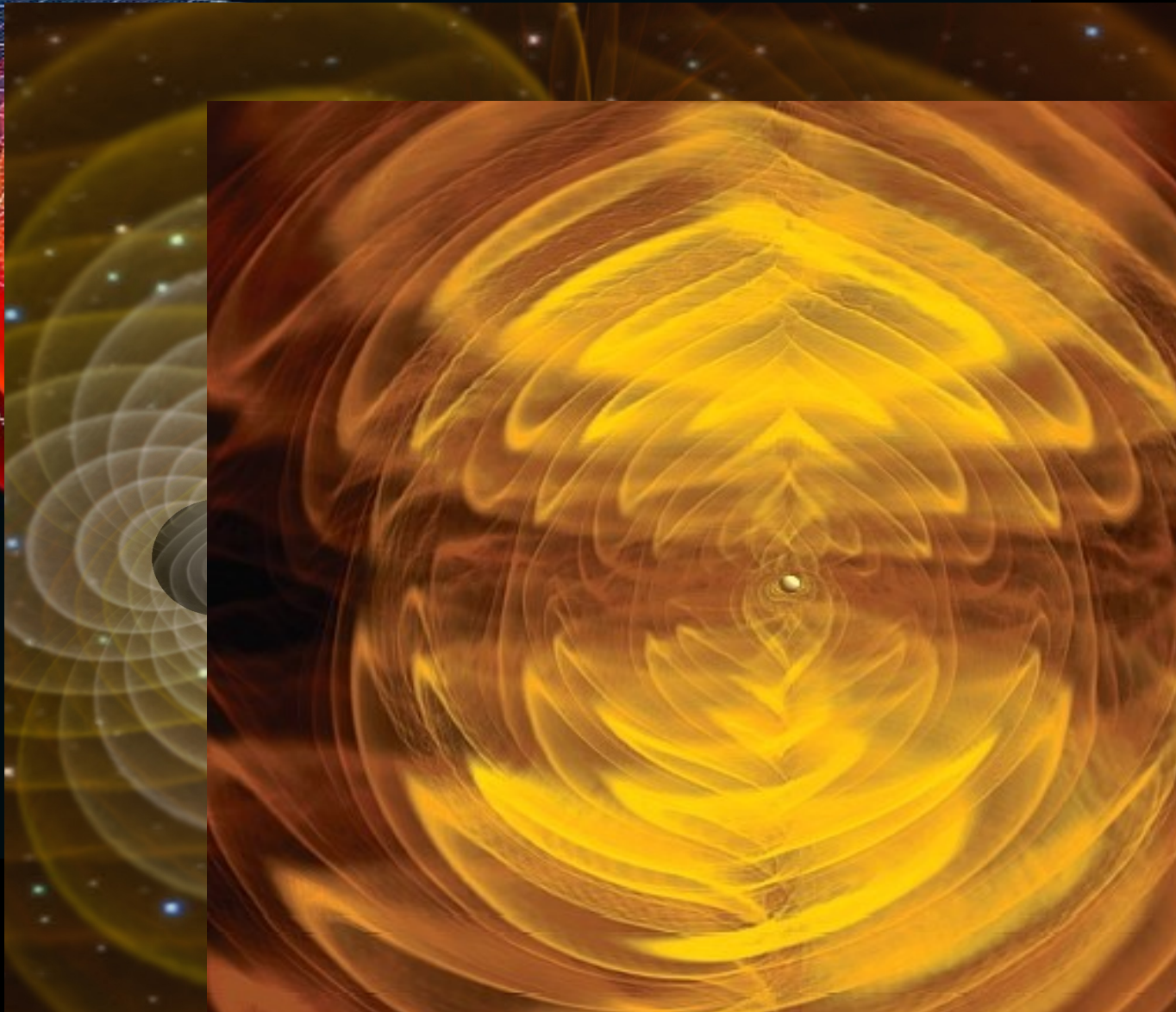
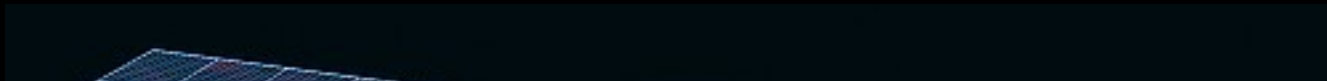
- 3+1 decomposition of the Einstein equations
- moving puncture technique on a refined mesh grid (gauge choice)

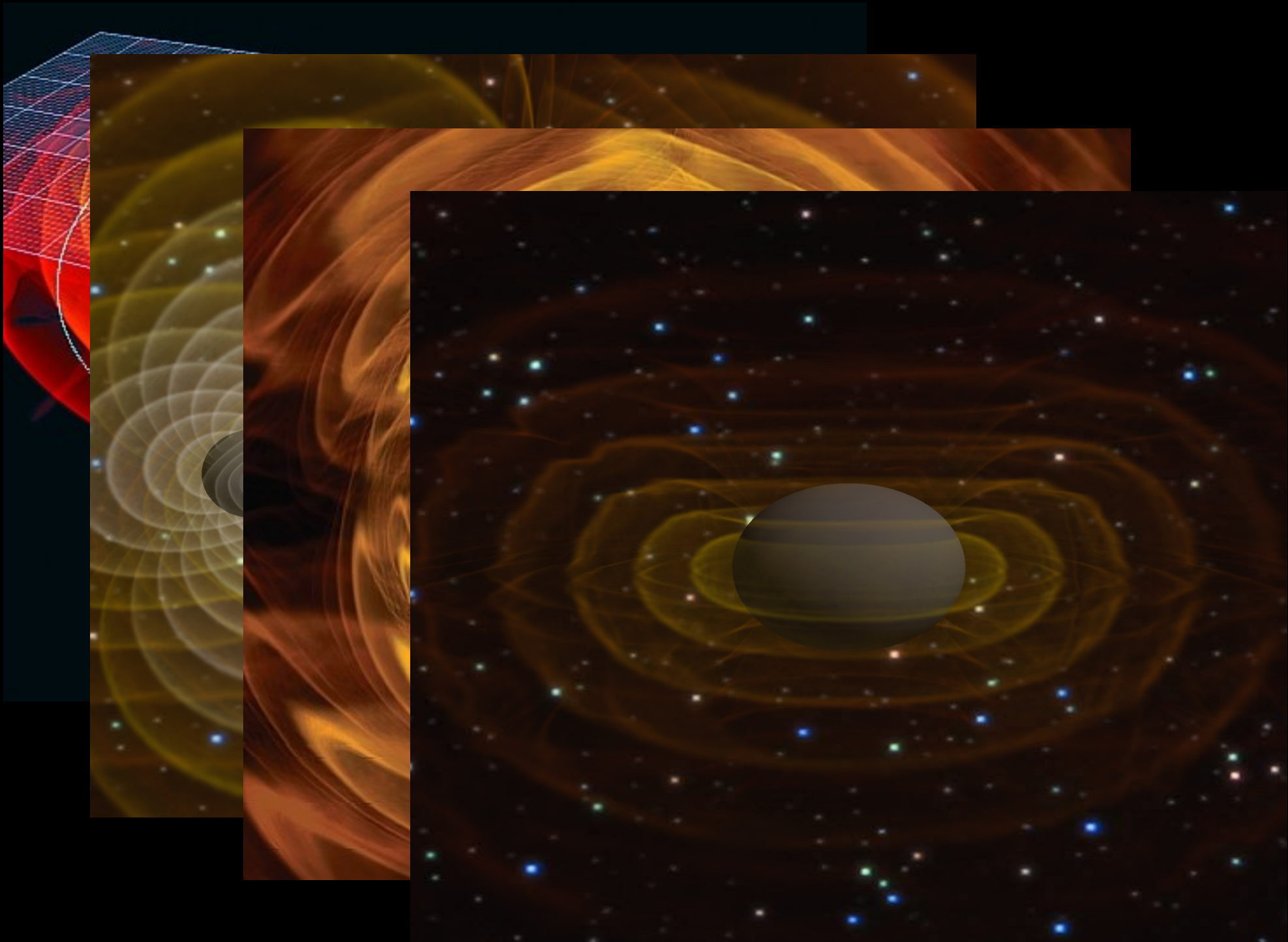
Since then, several groups (e.g. Goddard, Rochester, Caltech, AEI, Jena, etc...) started to produce full NR waveforms:

- mass ratio $0.1 < q \leq 1$
- spins up to 0.9, aligned or not
- circular or eccentric
- ~30 orbits+merger+ringdown

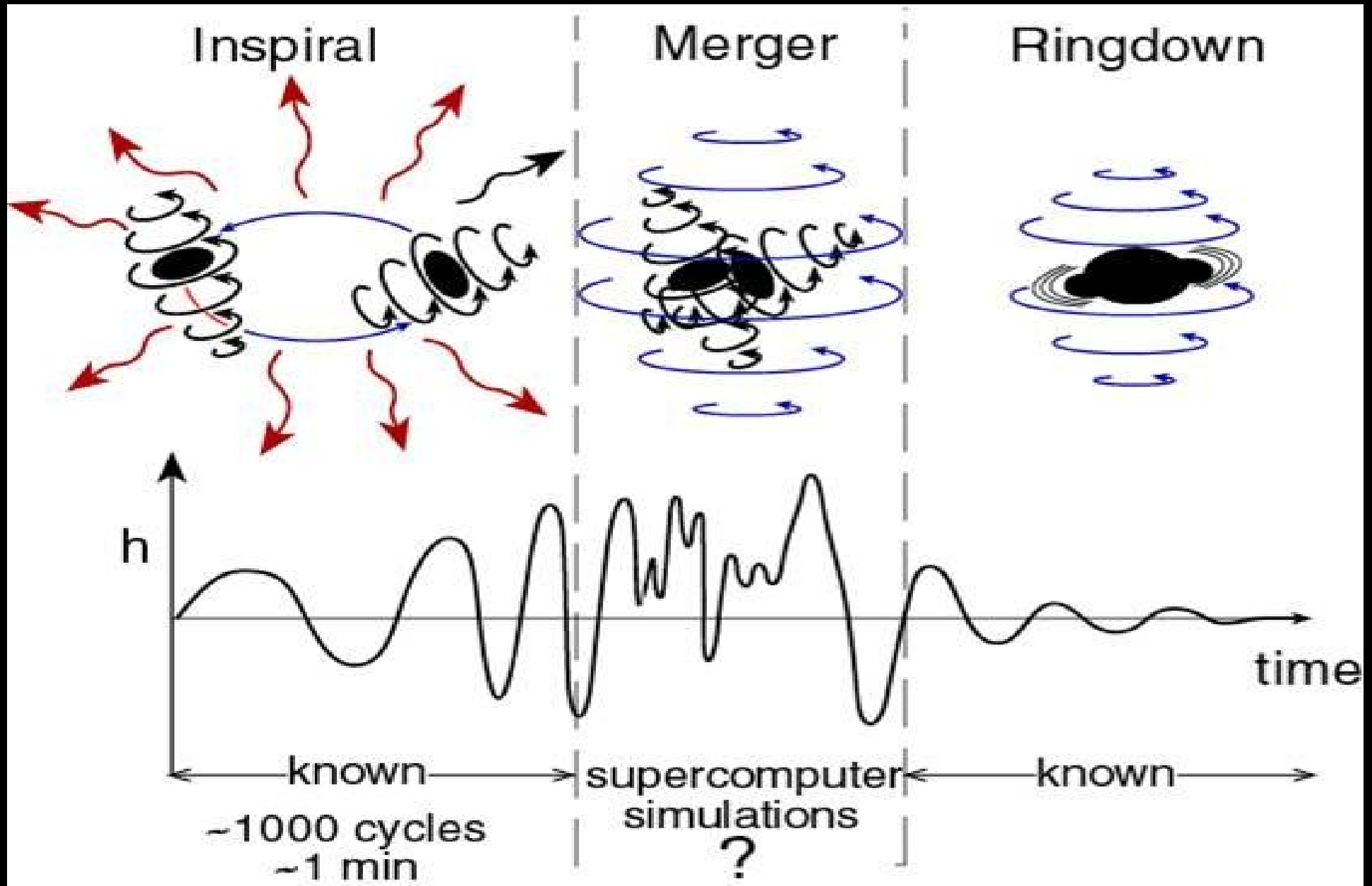




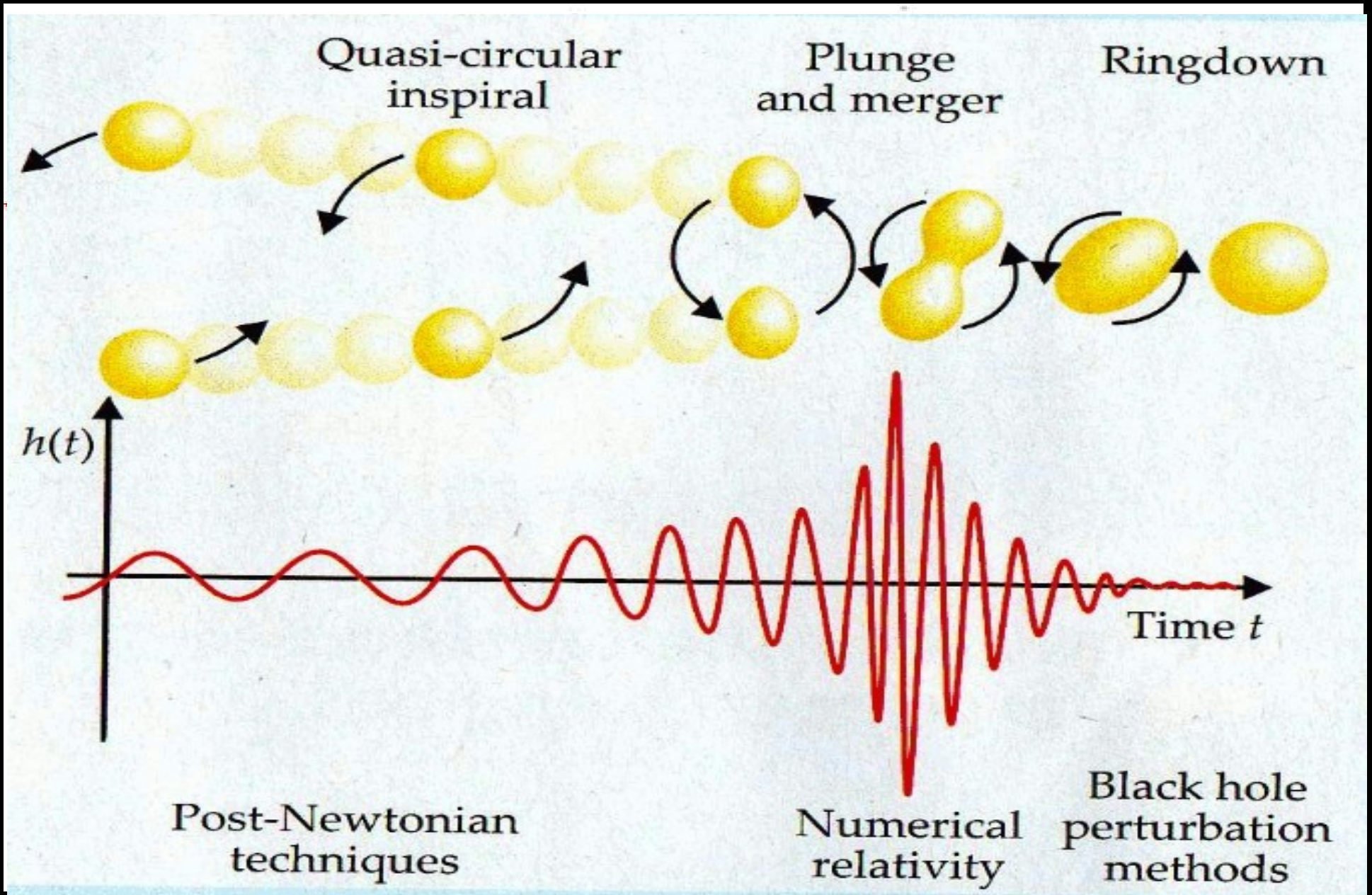




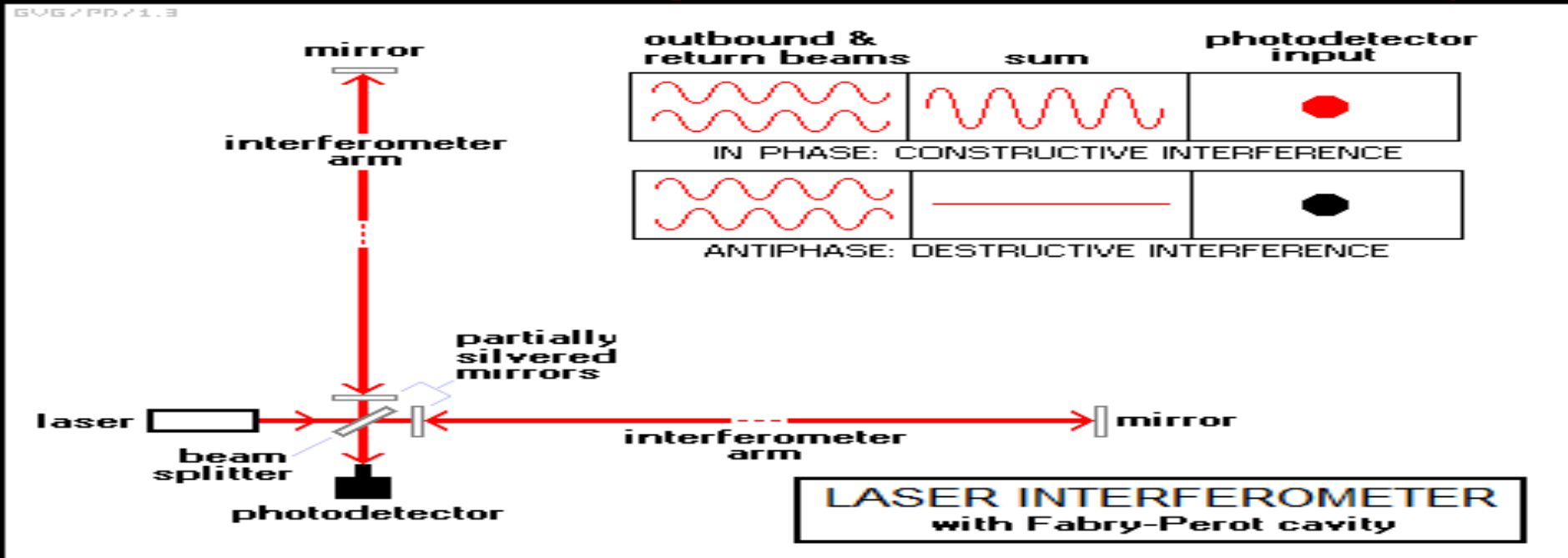
Can't wait to see what exciting non-linear phenomena we observe at the coalescence....



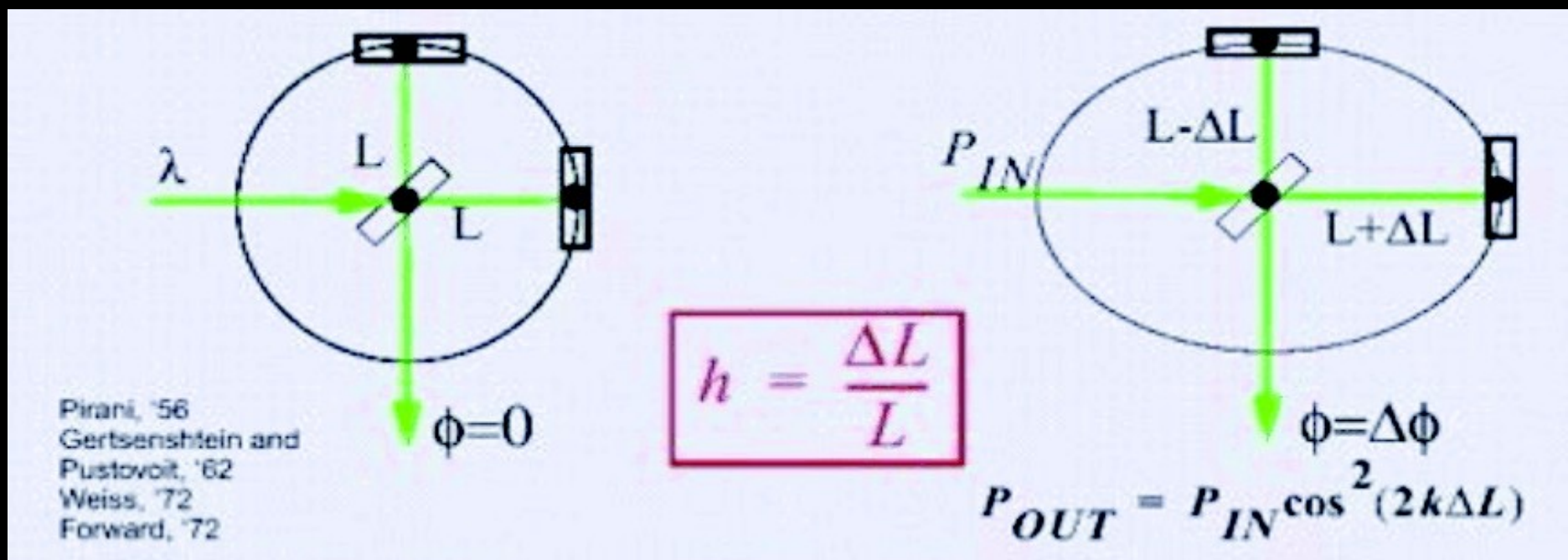
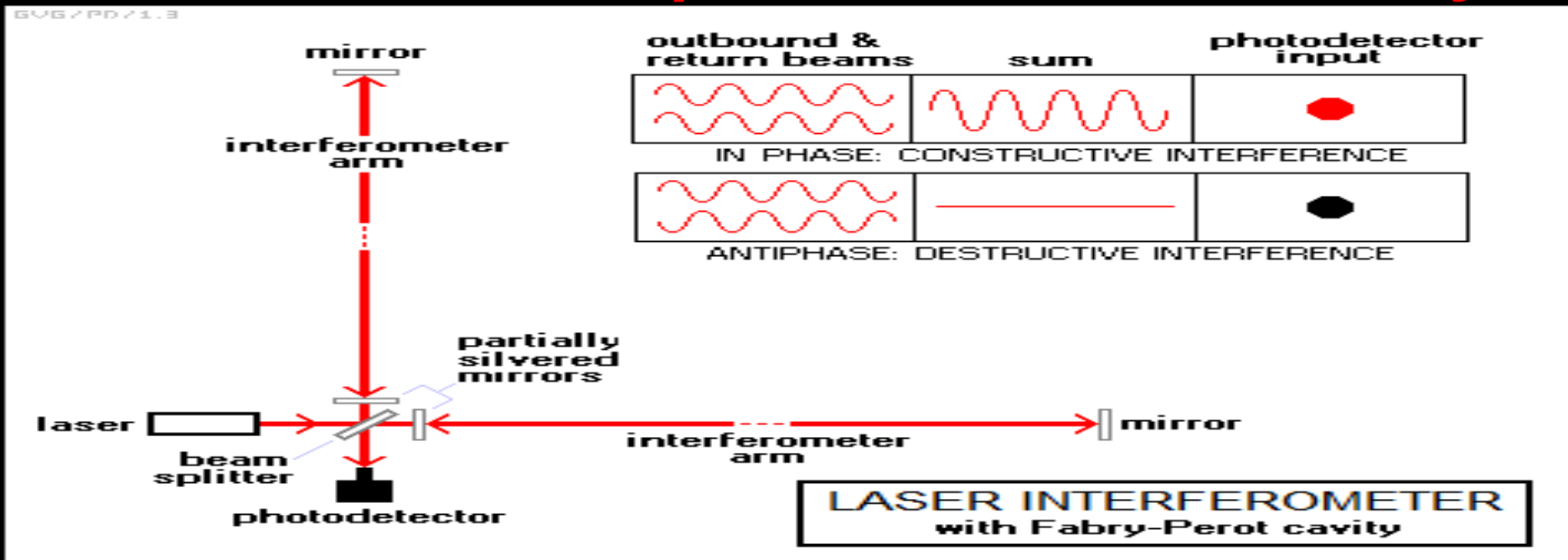
boooo...none, complete boredom...



Detection technique: laser interferometry



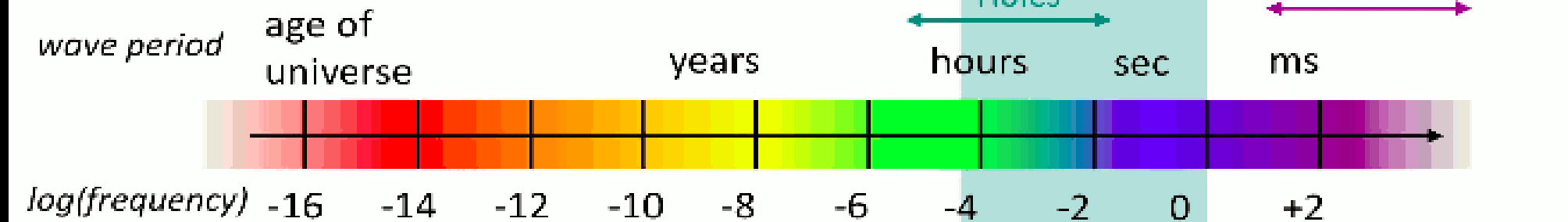
Detection technique: laser interferometry



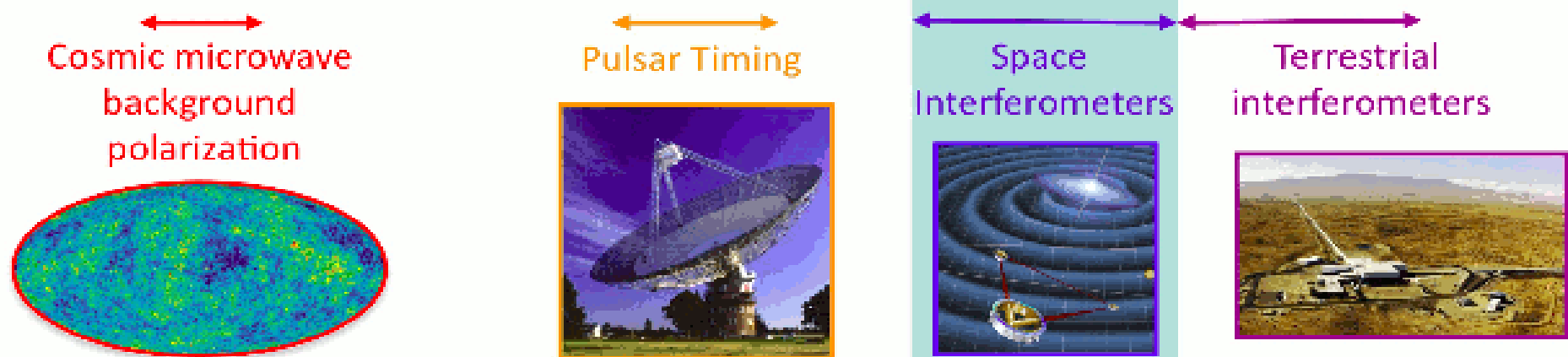
The passing wave changes the relative path of the photons in the two arms. This translates in a dephasing of the two laser beams that can be measured.

The gravitational wave spectrum

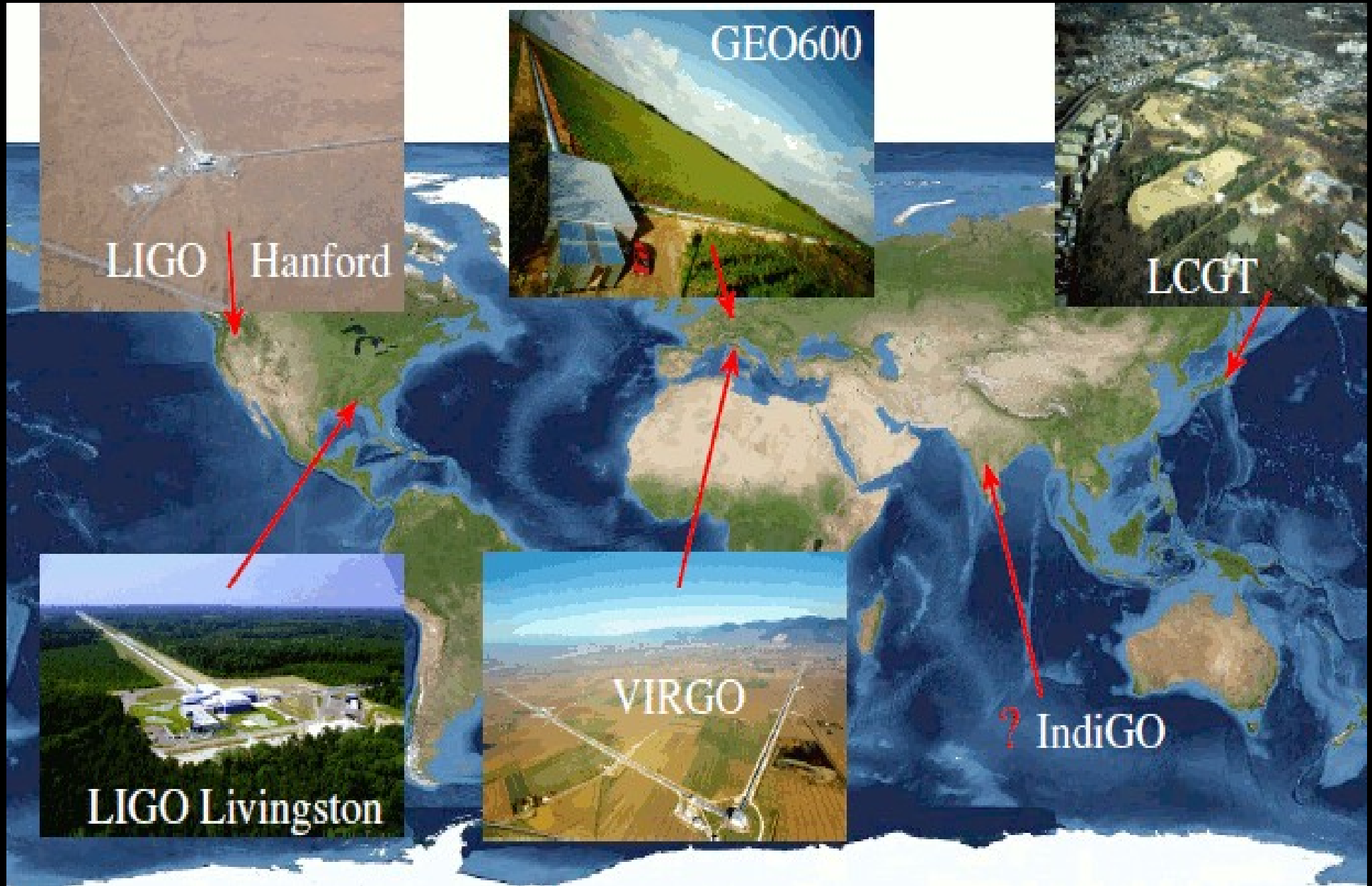
Sources



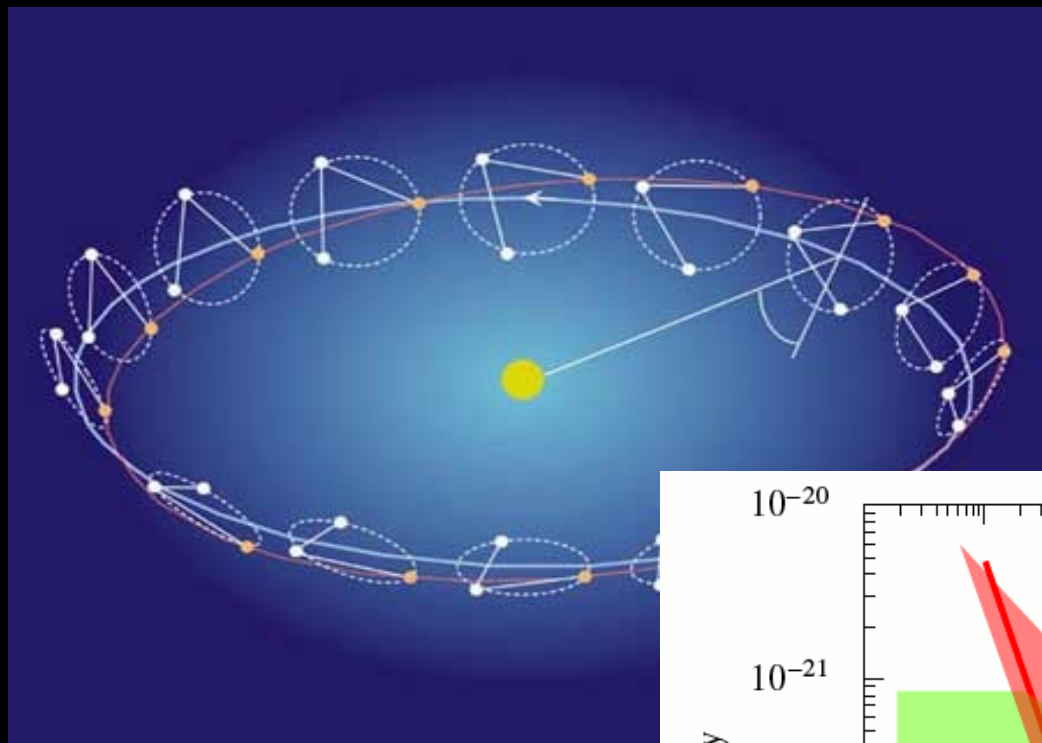
Detectors



The ground-based interferometer network



Interferometry in space: evolved Laser Interferometer Space Antenna

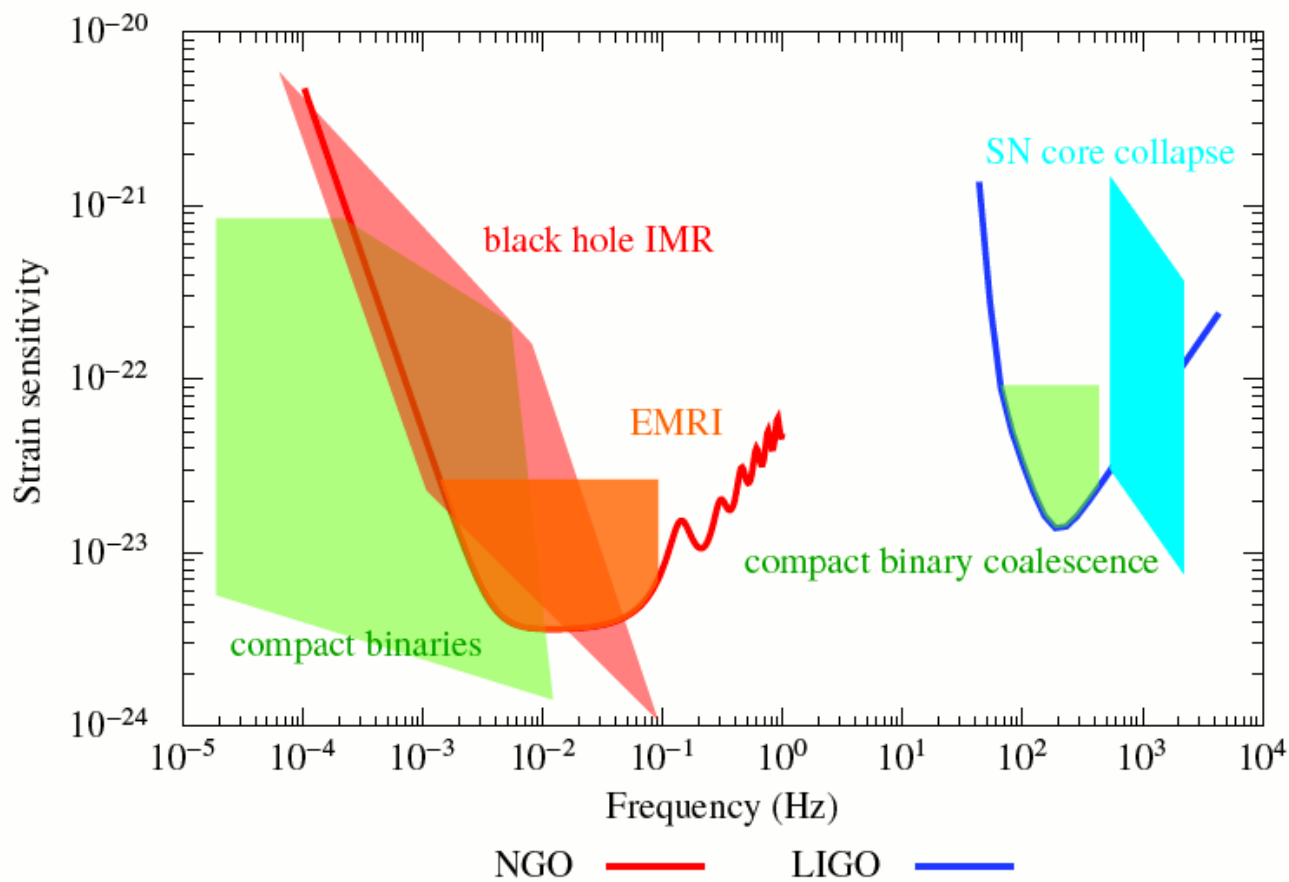


eLISA is sensitive at mHz frequency, where the evolution of MBHBs is fast.

eLISA will detect individual MBH binary inspirals!

eLISA

- same orbit as LISA
- 1Gm armlength
- four laser links
- >2 year lifetime
- launch <2022



The eLISA Revolution

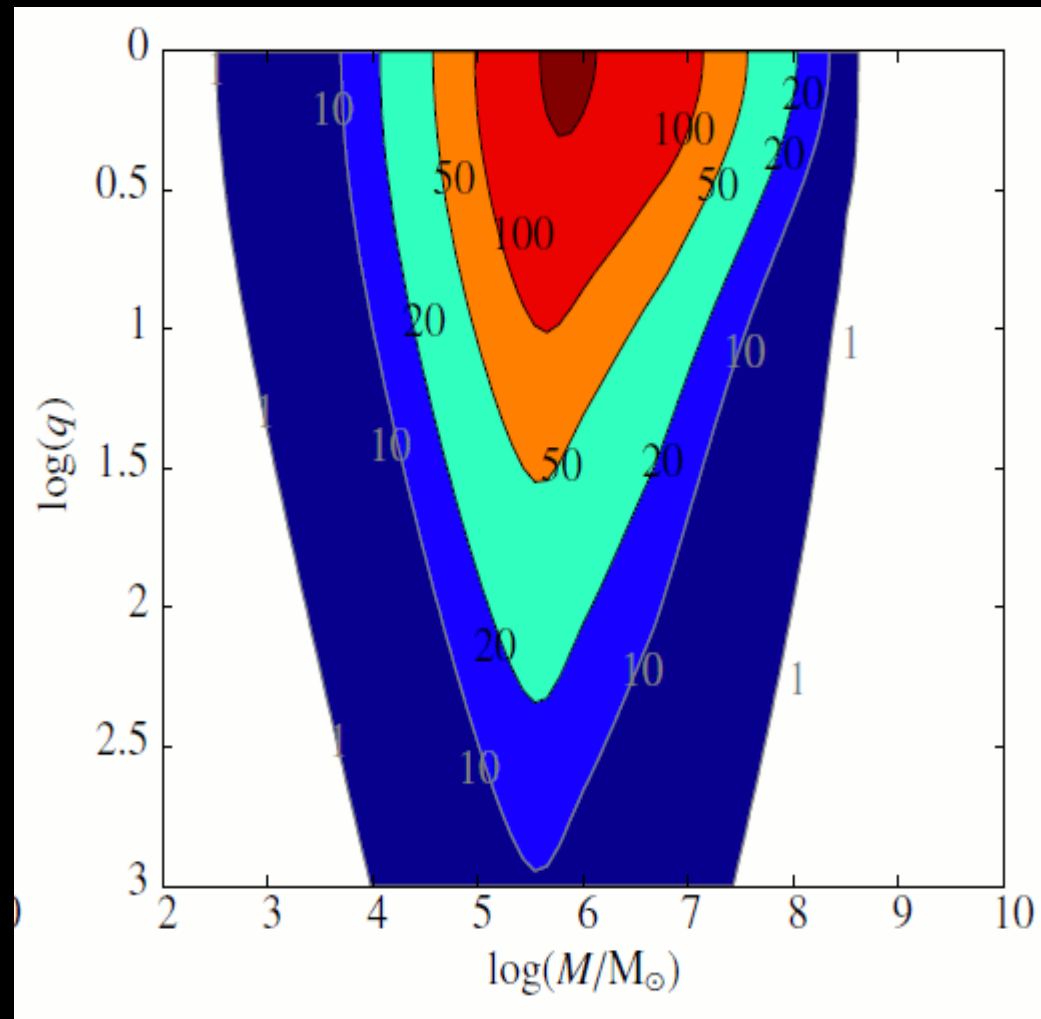
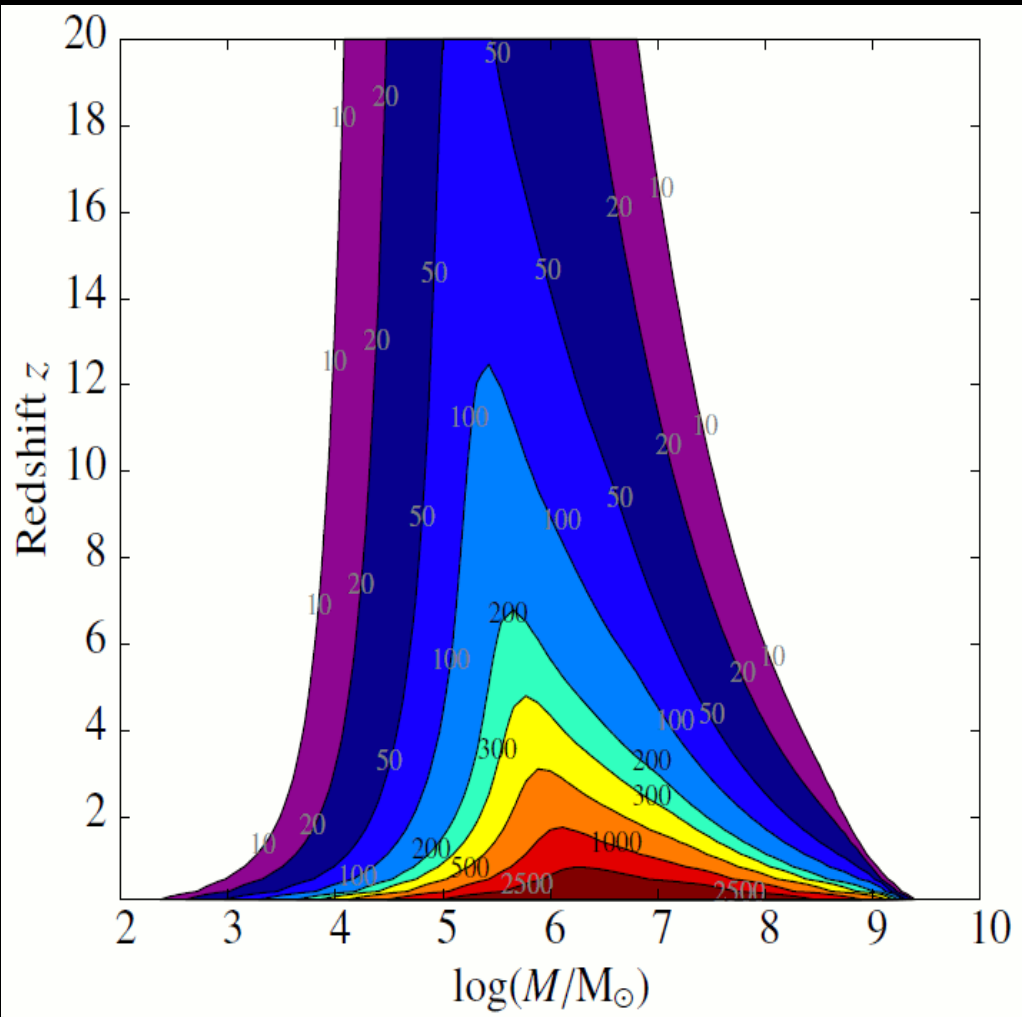
- Direct proof that massive central objects in galaxies are GR BHs
- Measurement of mass, spin of $10^6 M_{\odot}$ BHs at $z = 1$ to $\pm 1\%$
- Observation of universe before re-ionisation: BH mergers $z = 10-15$
- Reveal how massive BHs formed and evolved $z = 5-10$
- Tests of BH no-hair theorem, cosmic censorship
- Mass function of central black holes of ordinary galaxies to $z = 0.7$
- Study of stellar black hole clusters around central black holes
- Catalogue $> 10^3$ new white-dwarf binary systems in the Galaxy
- Precise masses and distances for dozens of white dwarf binaries
- Search for GWs from dilute population of cosmic strings and kinks
- Search for a stochastic GW background, especially constrain the EW phase transition
- Find IMBH by observing captures by central MBHs

The eLISA Revolution

- Direct proof that massive central objects in galaxies are GR BHs
- Measurement of mass, spin of $10^6 M_{\odot}$ BHs at $z = 1$ to $\pm 1\%$
- Observation of universe before re-ionisation: BH mergers $z = 10-15$
- Reveal how massive BHs formed and evolved $z = 5-10$
- Tests of BH no-hair theorem, cosmic censorship
- Mass function of central black holes of ordinary galaxies to $z = 0.7$
- Study of stellar black hole clusters around central black holes
- Catalogue $> 10^3$ new white-dwarf binary systems in the Galaxy
- Precise masses and distances for dozens of white dwarf binaries
- Search for GWs from dilute population of cosmic strings and kinks
- Search for a stochastic GW background, especially constrain the EW phase transition
- Find IMBH by observing captures by central MBHs

eLISA will observe the inspiral, merger and ringdown of MBH binaries in almost all the astrophysically relevant range, to high SNR!

SNR contour plot for an equal mass binary in the M - z plane



SNR contour plot for a binary at $z=4$ in the M - q plane

(Plots by E. Berti, non spinning PhenomC waveform used)

Source parameter extraction

$$h^{(\nu)}(t) = \frac{\sqrt{3}}{2} \left[F_+^{(\nu)}(t) h_+(t) + F_\times^{(\nu)}(t) h_\times(t) \right]$$

$$h_+ = 2 \frac{\mathcal{M}^{5/3}}{D_L} \left[1 + (\hat{\mathbf{L}} \cdot \hat{\mathbf{N}})^2 \right] (\pi f)^{2/3} \cos \phi(t)$$

$$h_\times = -4 \frac{\mathcal{M}^{5/3}}{D_L} (\hat{\mathbf{L}} \cdot \hat{\mathbf{N}}) (\pi f)^{2/3} \sin \phi(t),$$

$$F_+(\theta'_N, \phi'_N, \psi'_N) = \frac{1}{2} (1 + \cos \theta'^2_N) \cos 2\phi'_N \cos 2\psi'_N - \cos \theta'_N \sin 2\phi'_N \sin 2\psi'_N$$

$$F_\times(\theta'_N, \phi'_N, \psi'_N) = \frac{1}{2} (1 + \cos \theta'^2_N) \cos 2\phi'_N \sin 2\psi'_N + \cos \theta'_N \sin 2\phi'_N \cos 2\psi'_N$$

$$\begin{aligned} \phi(f) = \phi_c - \frac{1}{16} (\pi f \mathcal{M})^{-5/3} & \left[1 + \frac{5}{3} \left(\frac{743}{336} + \frac{11}{4} \eta \right) (\pi M f)^{2/3} - \frac{5}{2} (4\pi - \beta) (\pi M f) \right. \\ & \left. + 5 \left(\frac{3058673}{1016064} + \frac{5429}{1008} \eta + \frac{617}{144} \eta^2 - \sigma \right) (\pi M f)^{4/3} \right]; \end{aligned}$$

Detected signal: combination of the two wave **polarization amplitude** and the **antenna beam pattern**

polarization amplitude:

function of the source intrinsic parameters (M, f, ϕ), of the source distance D_L , and of the source inclination $i=L \cdot N$

Antenna pattern:

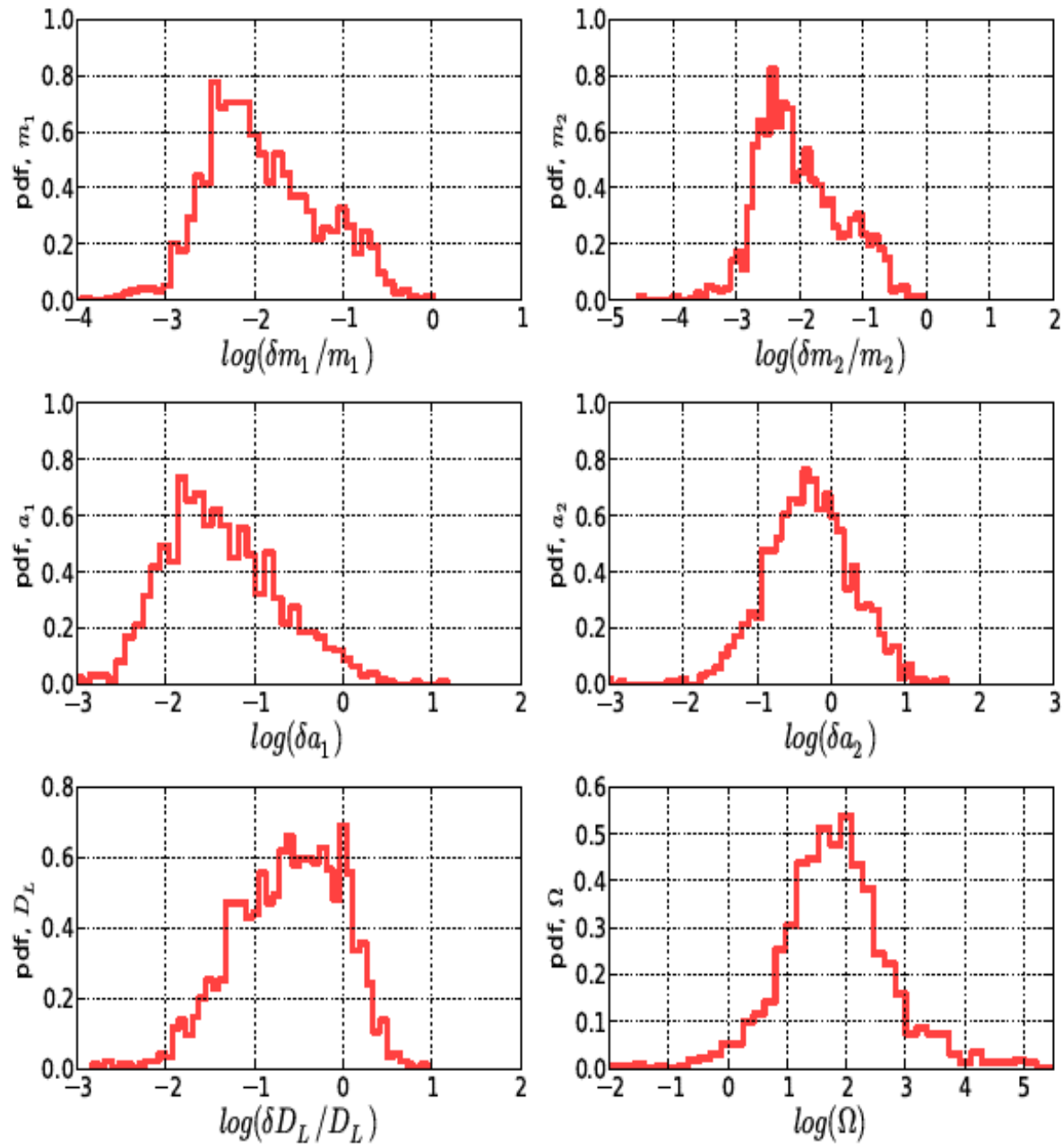
function of the relative source-detector orientation. Depends on: source sky location and polarization (θ, φ, ψ)

Phase evolution:

depends on the system masses and spins and eccentricity (M_1, M_2, a_1, a_2, e)

The full waveform for an eccentric spinning binary depends on **17 parameters**. Each of them leave a peculiar imprint in the waveform amplitude and phase.

What we can achieve: FIM results



We can measure:

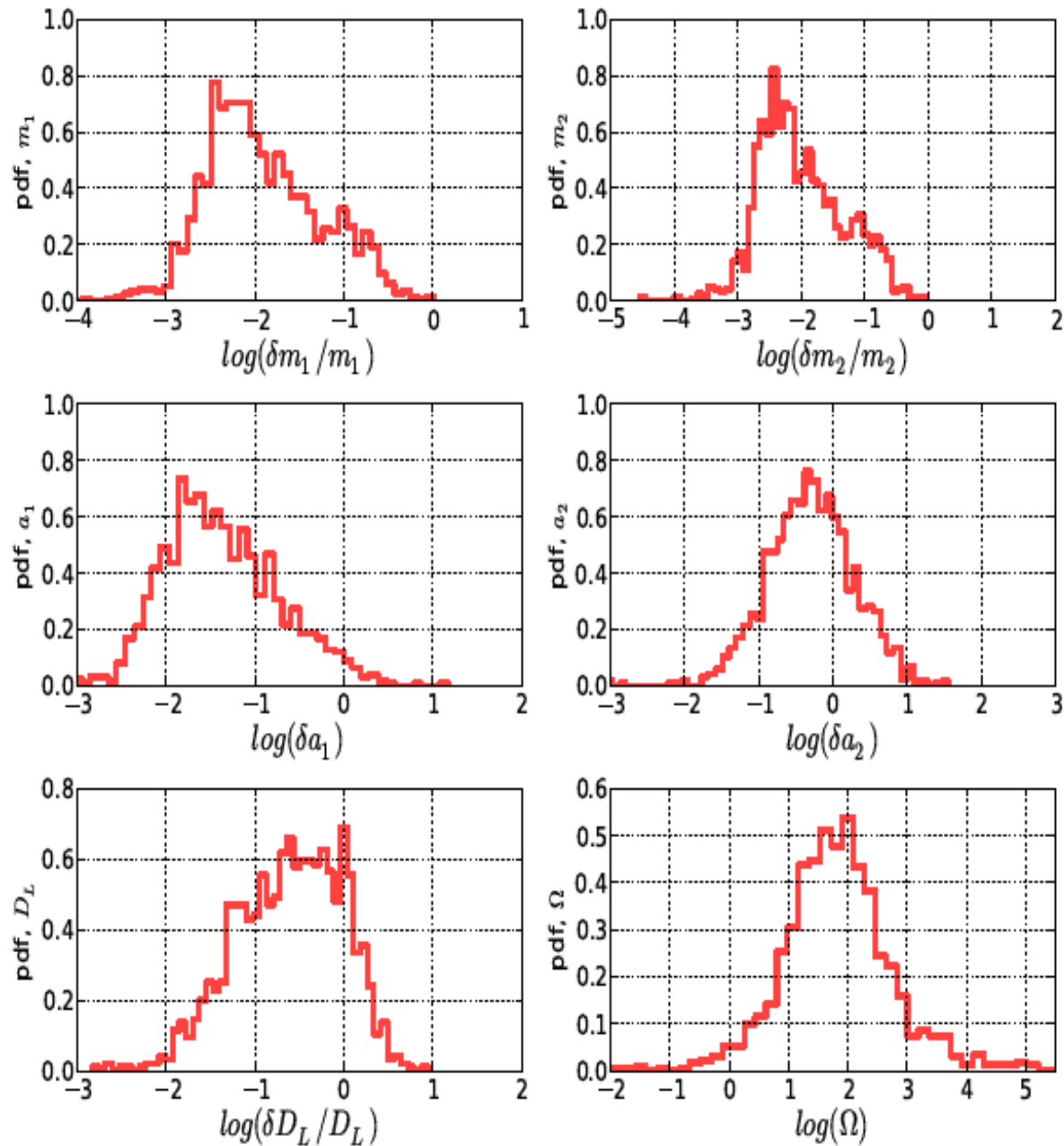
-Individual (redshifted) masses to **<1%** relative accuracy

-spin of the primary hole to **<0.1** (in many cases to **<0.01**)

-sky location to **10-1000 deg**
-luminosity distance to **10-100%**

(Results by N. Cornish, using spinning full IMR waveforms)

What we can achieve: FIM results



We can measure:

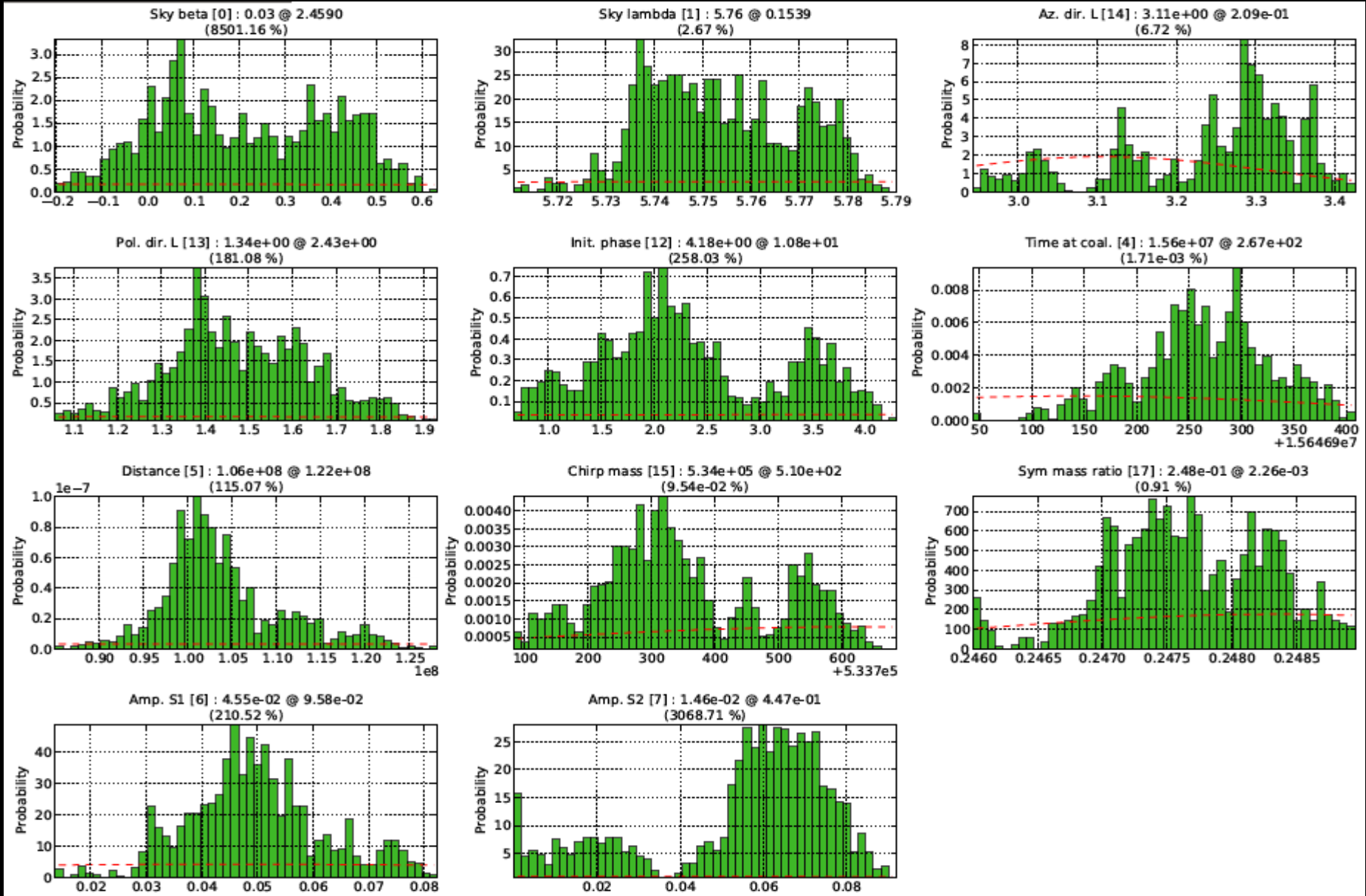
- Individual (redshifted) masses to $<1\%$ relative accuracy
- spin of the primary hole to <0.1 (in many cases to <0.01)
- sky location to 10-1000 deg
- luminosity distance to 10-100%

We cannot measure redshift.
Redshift can be extracted by D_L or via an EM counterpart

Potential problem: D_L accuracy degrades a lot for distant sources

(Results by N. Cornish, using spinning full IMR waveforms)

Beyond the FIM: full MCMC results



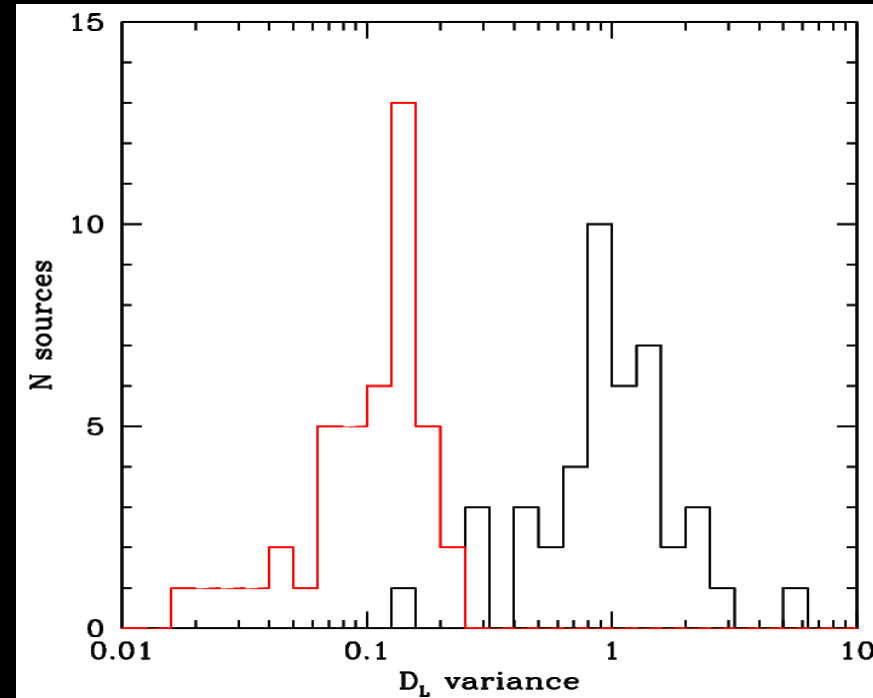
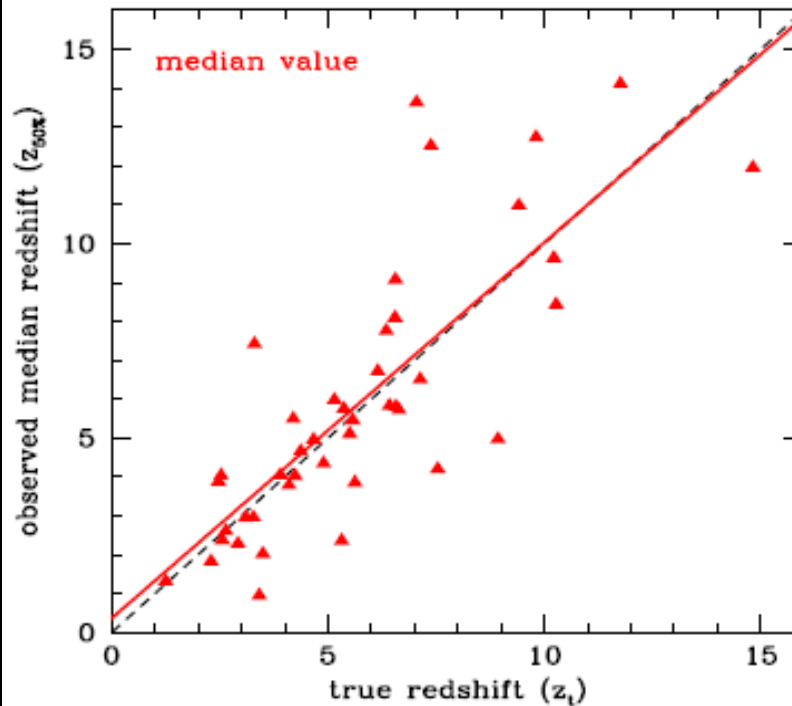
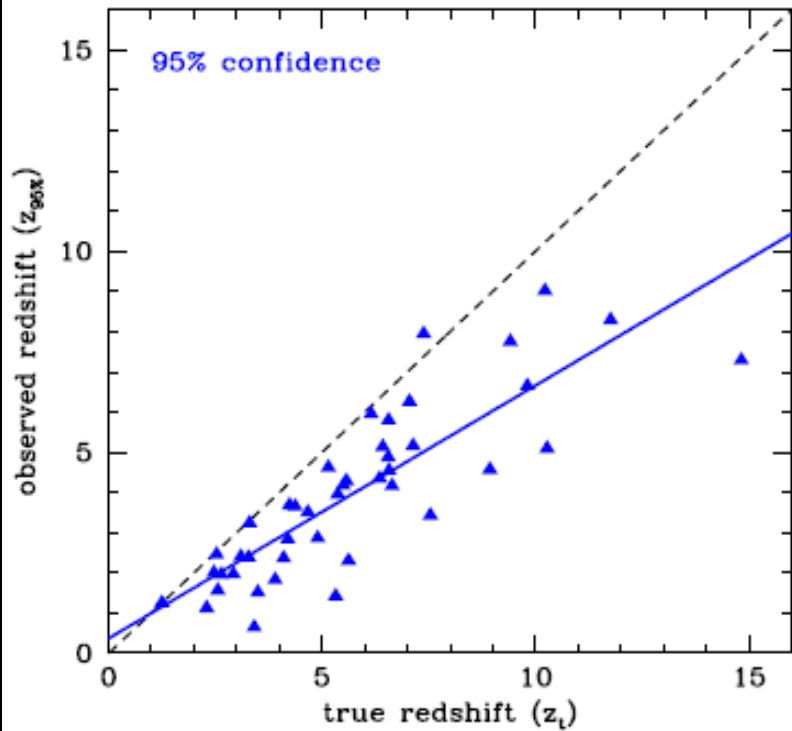
(Results by A. Petiteau, using spinning inspiral PN waveforms)

Source of $\sim 10^5 M_{\odot}$ @ $z \sim 10$, SNR ~ 15 : FIM would give $\sim 100\%$ distance error.

MCMC demonstrate that we can do much better

Test on 43 'bad' sources:
unfortunate sky location and/or very low SNR.

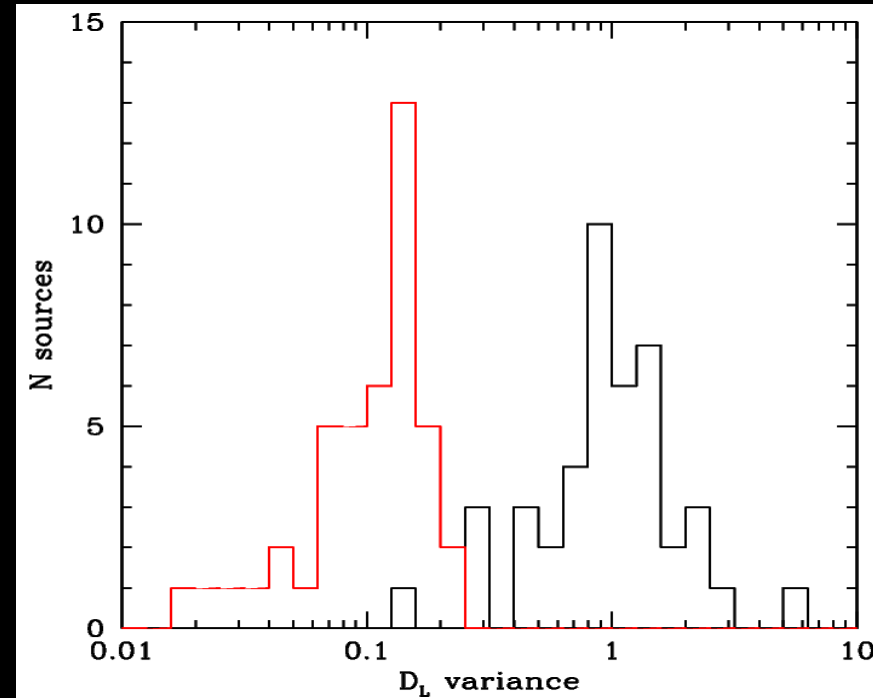
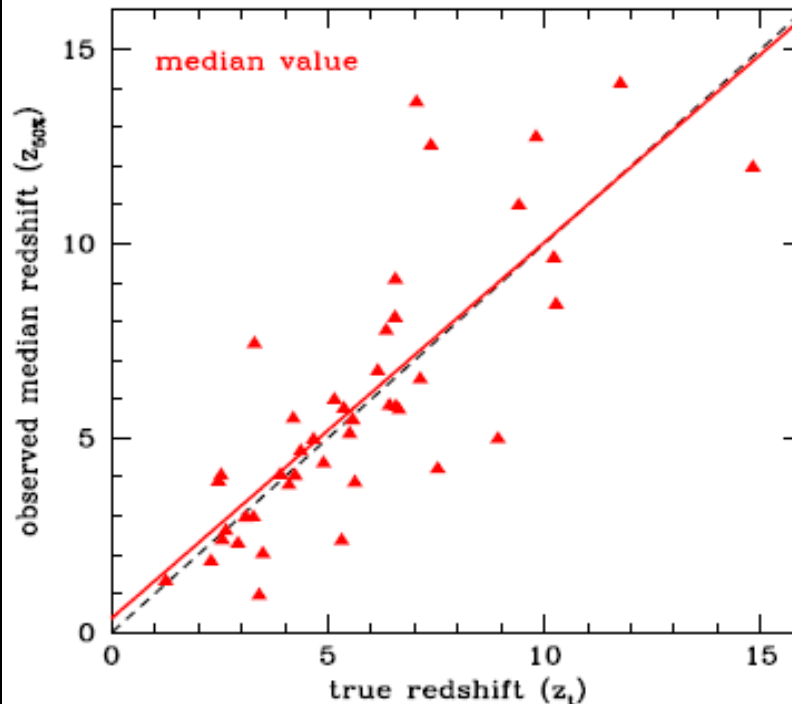
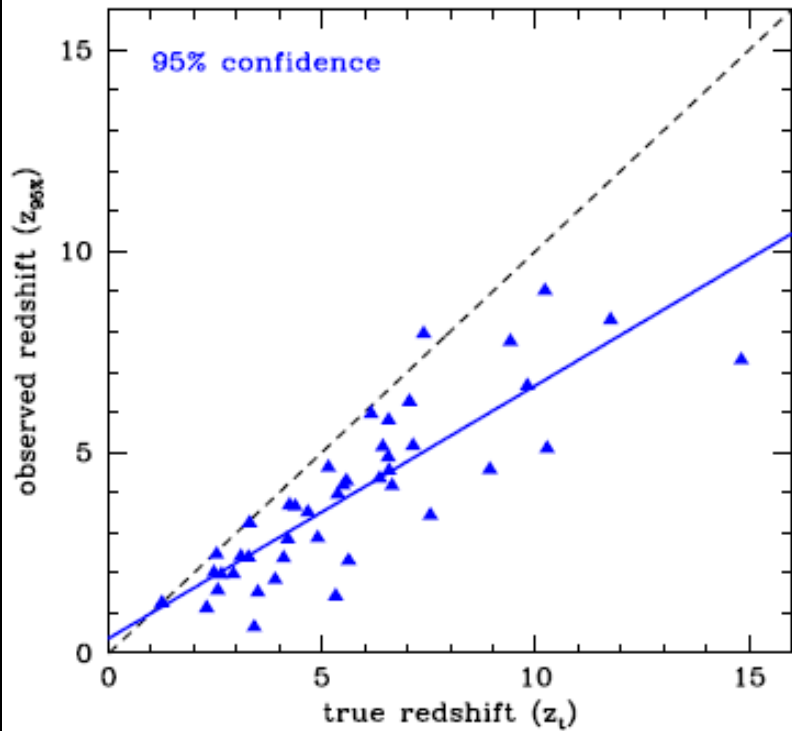
The FIM approximations work only for small Gaussian errors. In case of small SNR and non Gaussian posterior distributions, severely overestimates the uncertainties in the parameters



Even in such bad cases we can say that a source is at least at $2/3$ of its true redshift

Test on 43 'bad' sources:
unfortunate sky location and/or very low SNR.

The FIM approximations work only for small Gaussian errors. In case of small SNR and non Gaussian posterior distributions, severely overestimates the uncertainties in the parameters



Even in such bad cases we can say that a source is at least at 2/3 of its true redshift

Bottom line: we can see $z > 10$ events and actually tell that they are at $z > 10$!

A more complicated reality

When we search for sources, we 'match filter' the signal against a family of templates.

Full GR simulations are accurate but expensive:

- we can simulate only few cycles
- there is no way we will ever be able to cover a 17-dimensional parameter space!

A more complicated reality

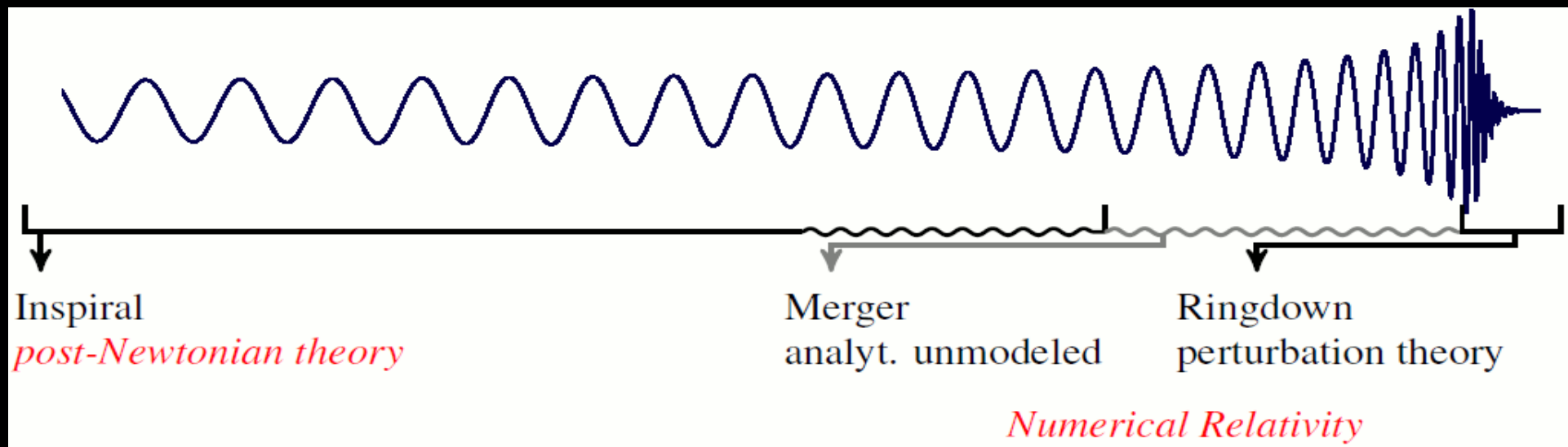
When we search for sources, we 'match filter' the signal against a family of templates.

Full GR simulations are accurate but expensive:

- we can simulate only few cycles
- there is no way we will ever be able to cover a 17-dimensional parameter space!

Full simulations will be used only to calibrate parametric families of templates:

- Hybrid waveforms**: stitch together PN inspiral to full GR merger and ringdown
- Effective one body waveforms (EOB)**: analytical waveforms extracted by an effective general relativistic Hamiltonian, to be calibrated against NR simulations.



A more complicated reality

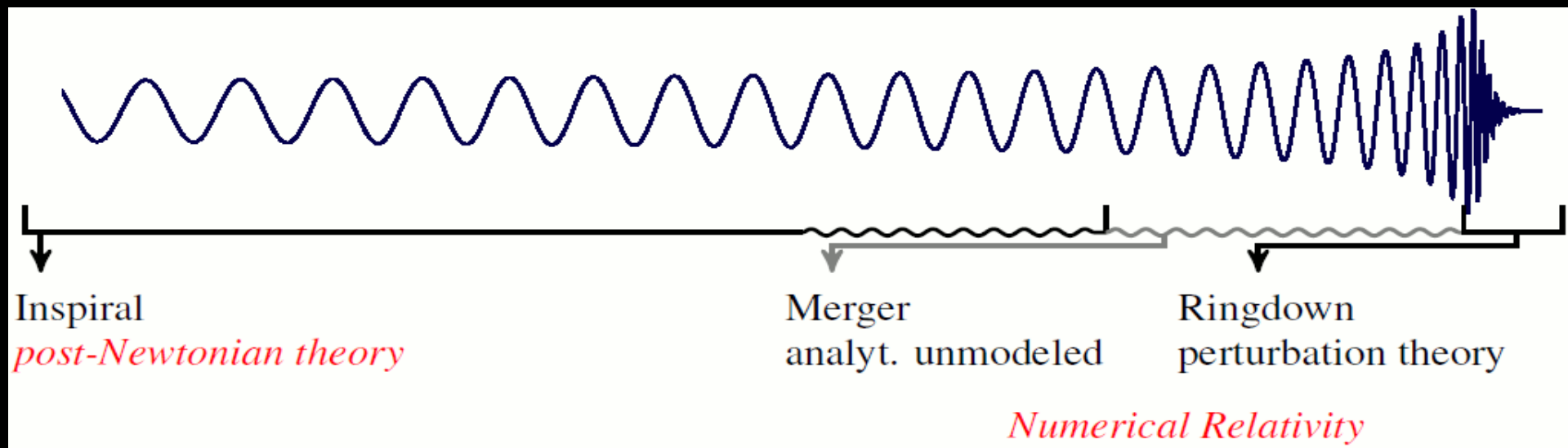
When we search for sources, we 'match filter' the signal against a family of templates.

Full GR simulations are accurate but expensive:

- we can simulate only few cycles
- there is no way we will ever be able to cover a 17-dimensional parameter space!

Full simulations will be used only to calibrate parametric families of templates:

- Hybrid waveforms**: stitch together PN inspiral to full GR merger and ringdown
- Effective one body waveforms (EOB)**: analytical waveforms extracted by an effective general relativistic Hamiltonian, to be calibrated against NR simulations.



Hybrid and EOB models are not unique!
we have different family of templates
non of them will actually 'match' the real GW signal

Does such match filtering make sense at all?

Hybrid can be constructed using different PN expansions. Thus producing slightly different waveforms.

Let's take a particular source and construct two different hybrid waveforms: h and g . The mismatch is defined as $M=1-\langle h,g \rangle$. M measures how 'different' are two waveforms. And the signal recovery rate goes with $(1-M)^3$.

For different PN approximations $M \sim 0.2$ implying a recovery rate $\sim 50\%$. BAD!

However what makes sense is the comparison between 'families of templates' not between two individual template. The waveform h , can be well matched by a waveform g' with slightly different source parameters.

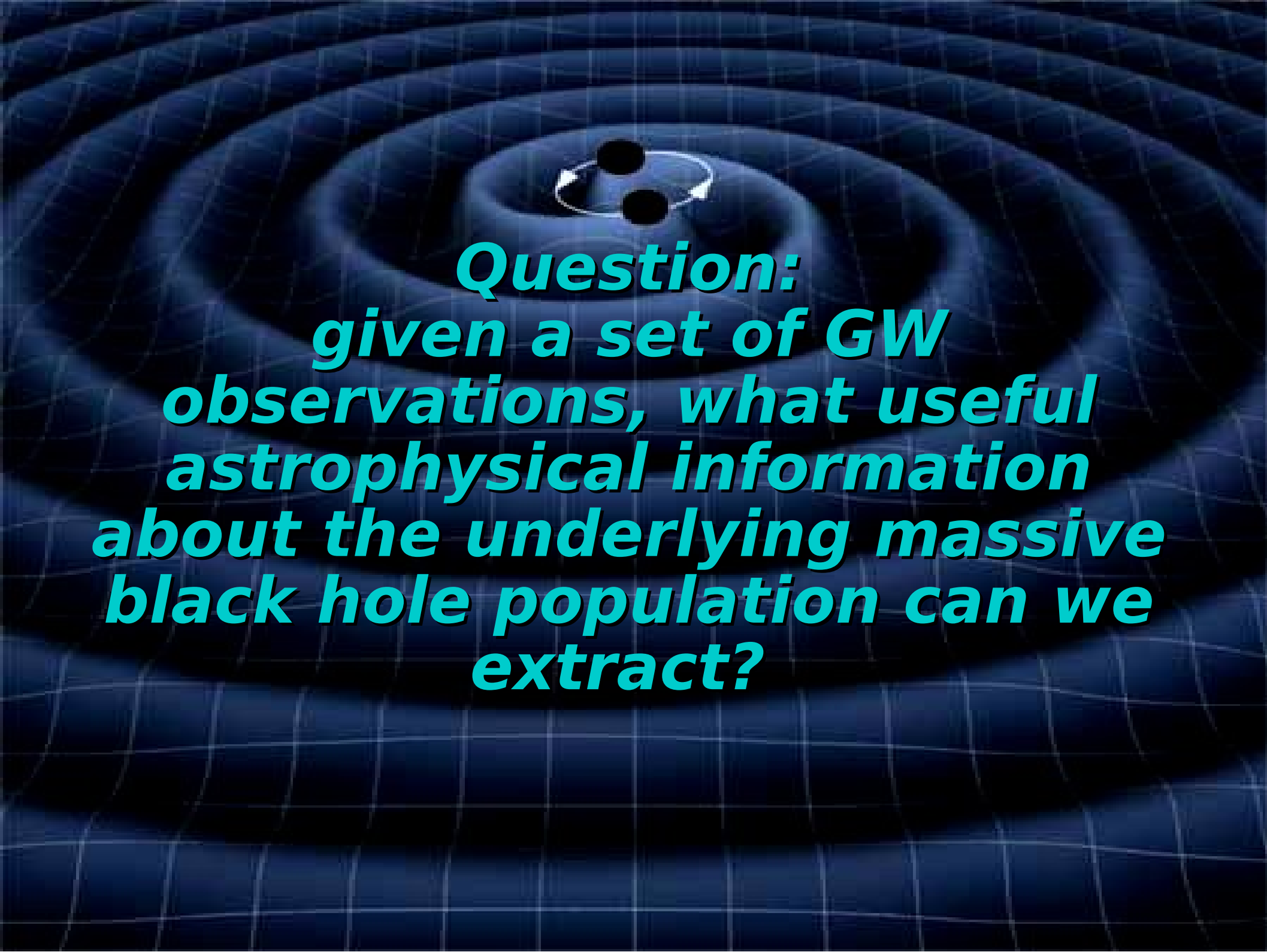
It turns out than the mismatch $M=1-\langle h,g' \rangle$ is $\sim 10^{-3}$, and the introduced error in the parameters is $<1\%$ in the source masses and <0.1 in the spins.

This means that even if we are searching signals with a template family that is an approximation of the true GR waveforms:

- 1-We will be able to find basically all the signals
- 2-We will be able to estimate the source parameters without introducing any severe bias

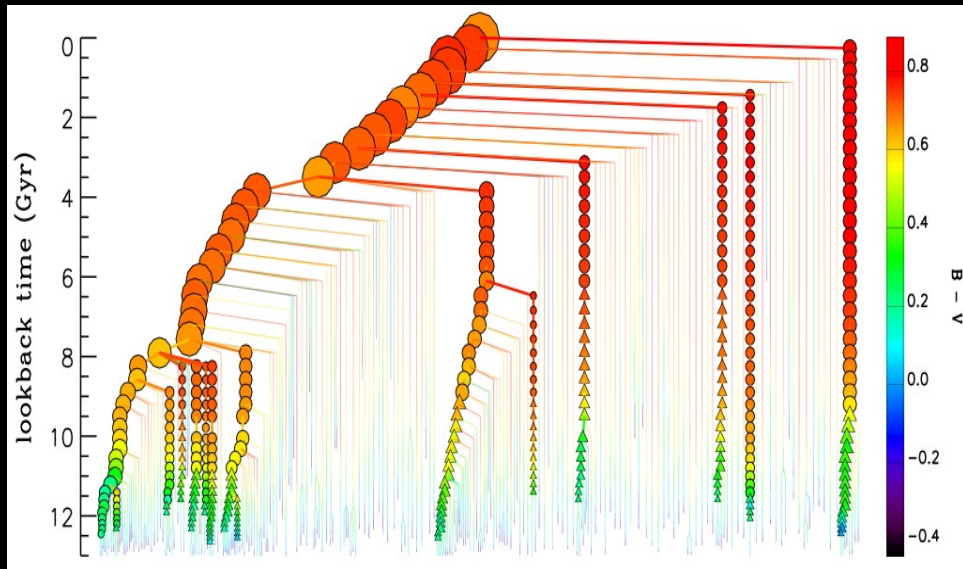
eLISA will give us:

- Individual (redshifted) masses to $<1\%$ relative accuracy**
- spin of the primary hole to <0.1 (in many cases to <0.01)**
- sky location to 10-1000 deg**
- luminosity distance to $<10\%$ in most cases**

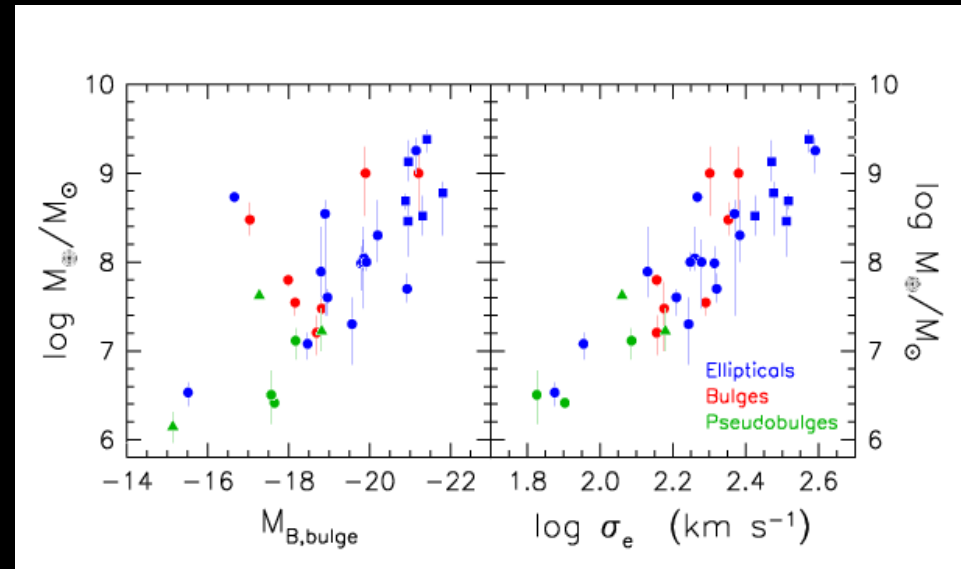


***Question:
given a set of GW
observations, what useful
astrophysical information
about the underlying massive
black hole population can we
extract?***

Structure formation in a nutshell

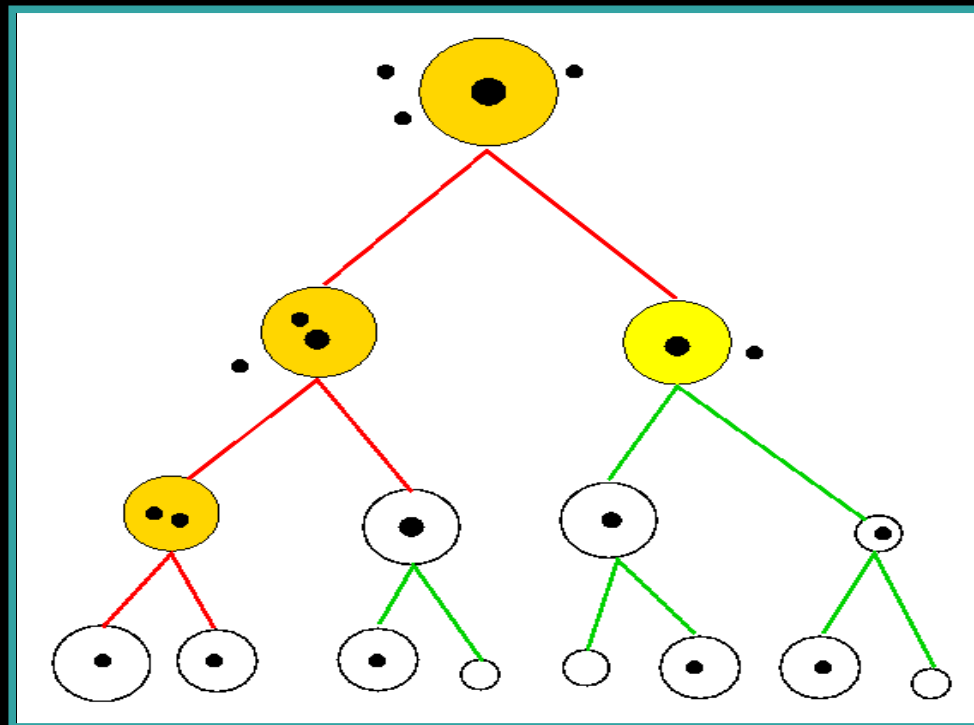


From De Lucia et al 2006



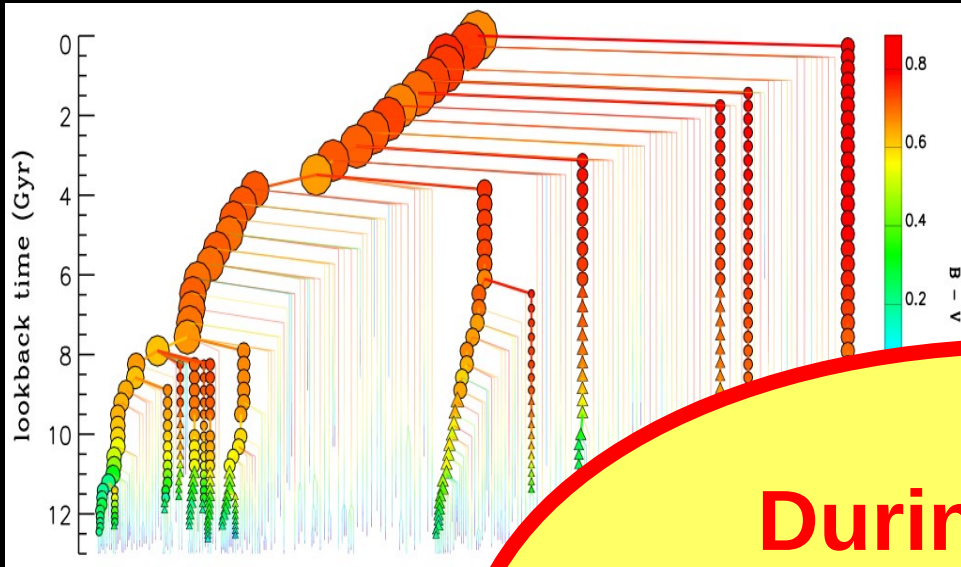
Ferrarese & Merritt 2000, Gebhardt et al. 2000

==



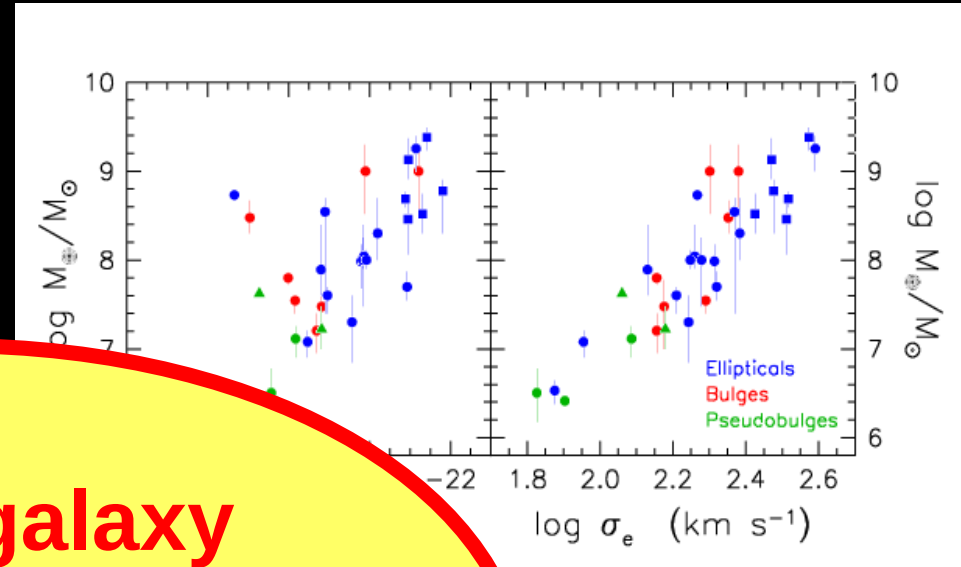
Volonteri Haardt & Madau 2003

Structure formation in a nutshell



From De Lucia et al 2007

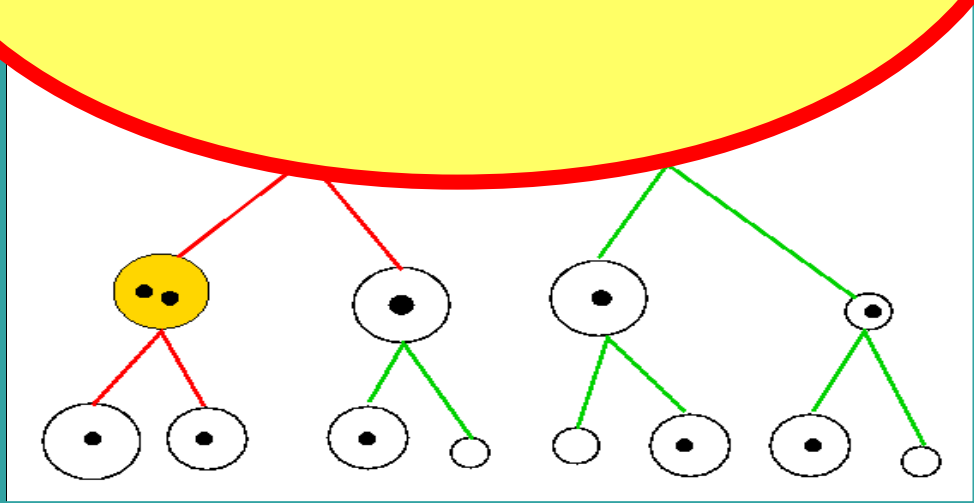
+



Gebhardt et al. 2000

During galaxy mergers, MBHBs will inevitably form!

=



Volonteri Haardt & Madau 2003

Hierarchical MBH growth

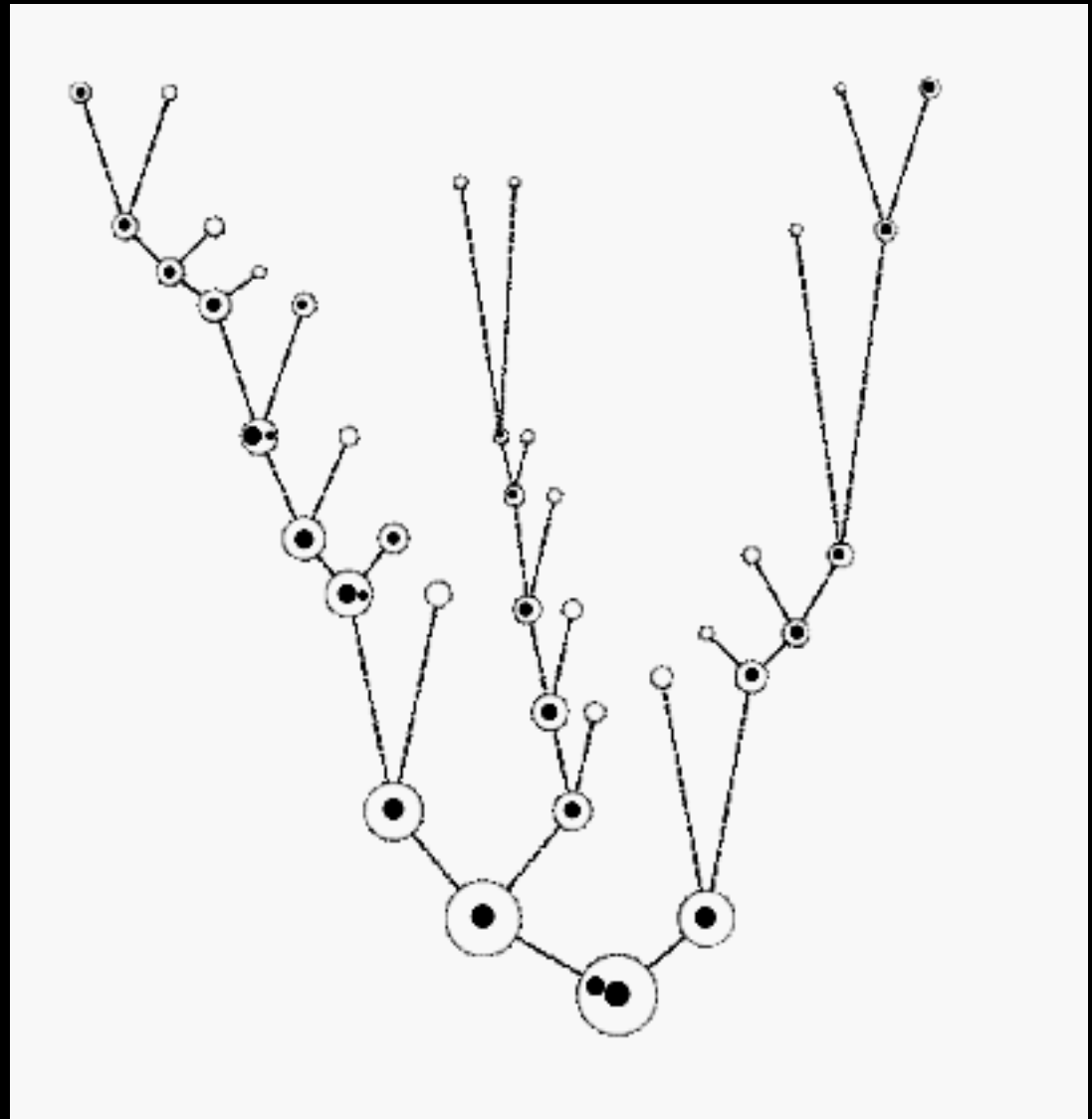
THE MODEL

MBHS are grown from *seeds* BHs. These seeds are incorporated in larger and larger halos, *accreting gas and interacting each with other after mergers.*

OBS. CONSTRAINTS:

1. LF of quasars
2. X-ray unresolved bkg
3. M_{BH} -bulge relations
4. Local MBH MF
5. Galactic cores

(Volonteri, Haardt & Madau 2003)



Massive black hole binaries

We consider 4 different formation models differing in:

- 1- MBH seeding mechanism (small vs large seeds)
- 2- Accretion geometry (efficient vs chaotic)

Models are named after the LISA PE taskforce paper:

- 1-SE: small seeds+efficient accretion
- 2-SC: small seeds+chaotic accretion
- 3-LE: large seeds+efficient accretion
- 4-LC: large seeds+chaotic accretion

Model	Detector	1 int. SNR= 8	1 int. SNR= 20	2 int. SNR= 8	2 int. SNR= 20
SE	LISA	64.96	40.98	79.73	49.96
	C2	40.09	23.01	49.73	29.89
	C1	32.40	17.79	40.66	23.58
SC	LISA	70.64	46.99	84.76	56.19
	C2	45.63	27.04	55.50	34.99
	C1	37.54	20.84	46.38	27.86
LE	LISA	48.70	46.04	49.19	48.56
	C2	44.94	34.62	47.80	42.11
	C1	41.61	27.50	46.07	35.88
LC	LISA	42.80	40.47	43.16	42.43
	C2	38.72	30.47	41.21	36.00
	C1	35.30	25.04	38.81	31.19

PROCEDURE

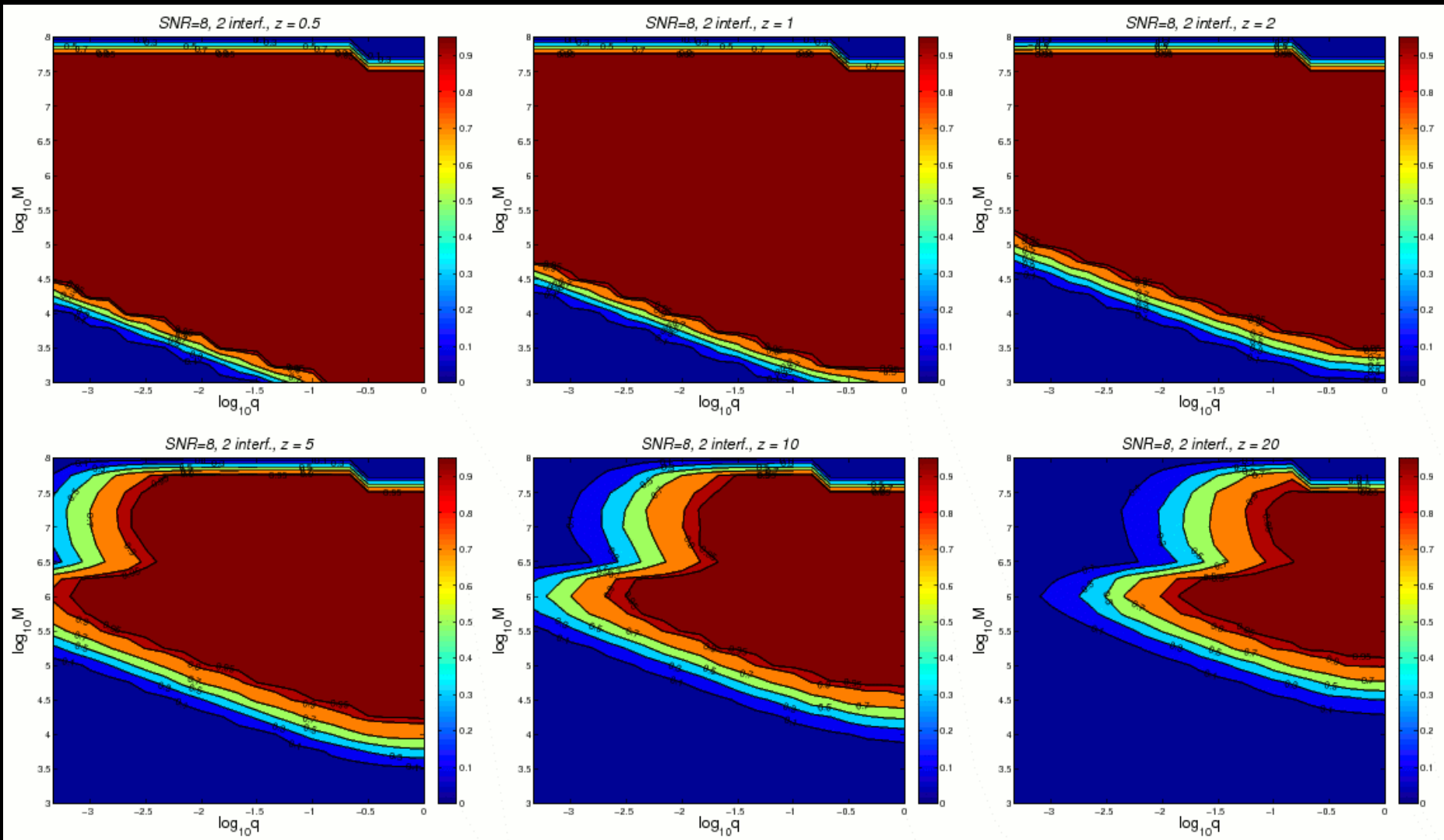
- a-Construct the detector transfer function (takes into account for the adopted waveform and for the detector performance)
- b-Filter the theoretical distribution through the transfer function to produce the “theoretically observable” distribution
- c-Perform Montecarlo realizations of the MBH population
- d-Create catalogs of observed binaries including FIM errors from LISA observations and compare observations with theoretical models

We compare:

- the 4 pure models described before through the odds ratio
- artificially mixed models of the form $N_{mix} = f_1 N_1 + \dots + f_n N_n$
we find the maximum of the posterior distribution in the mixing parameter space

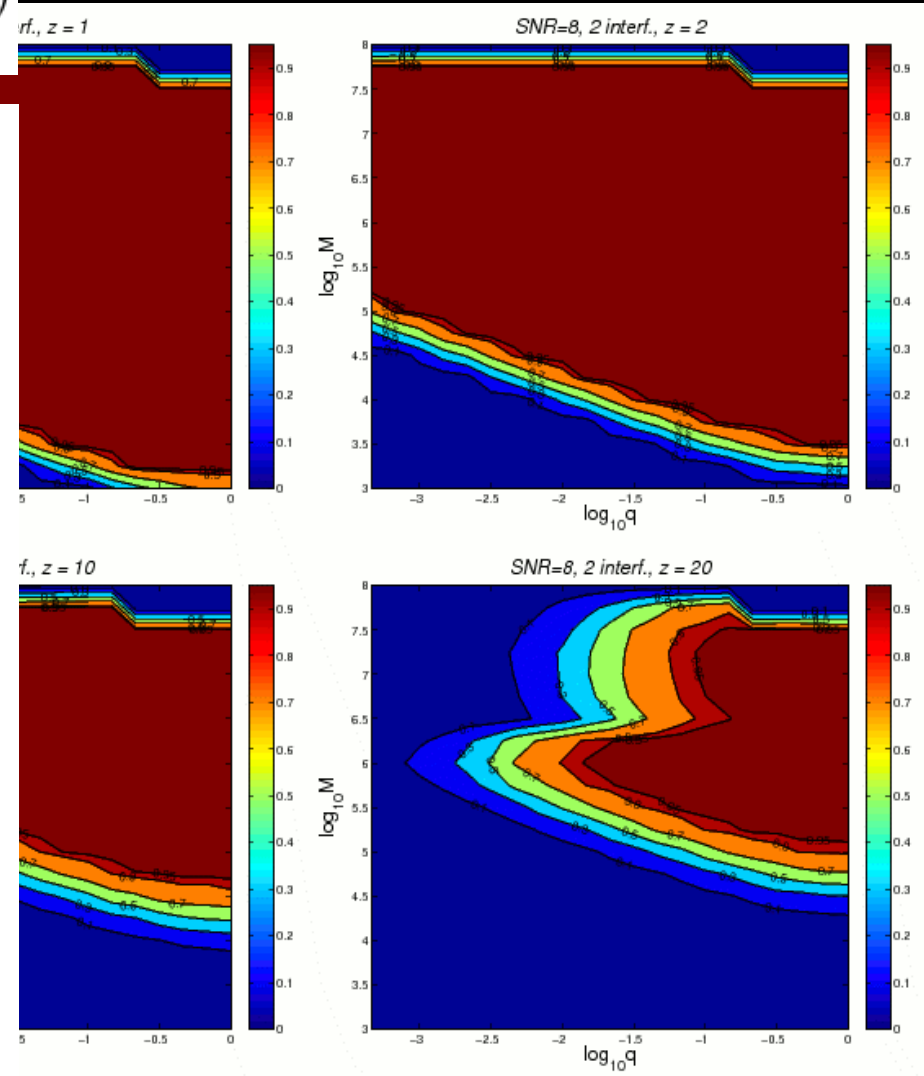
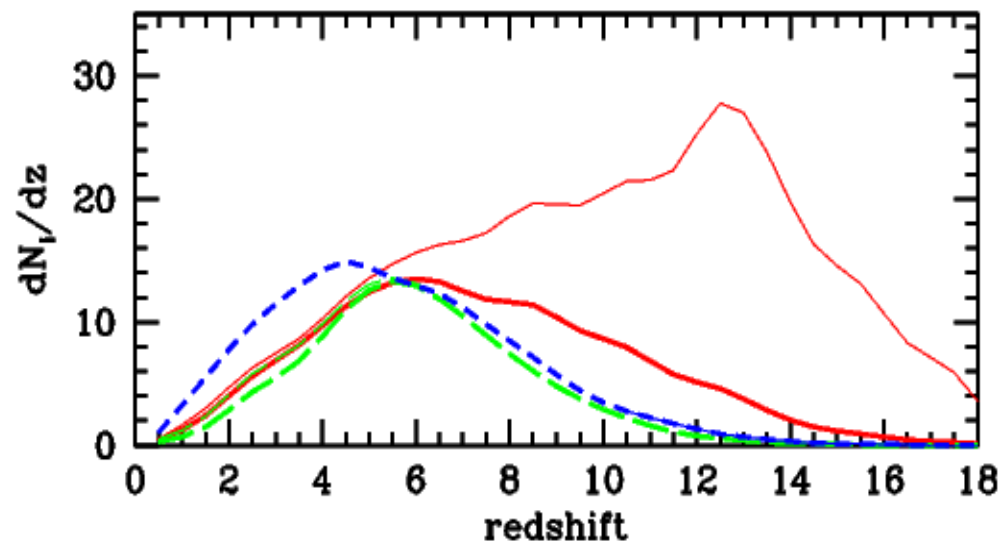
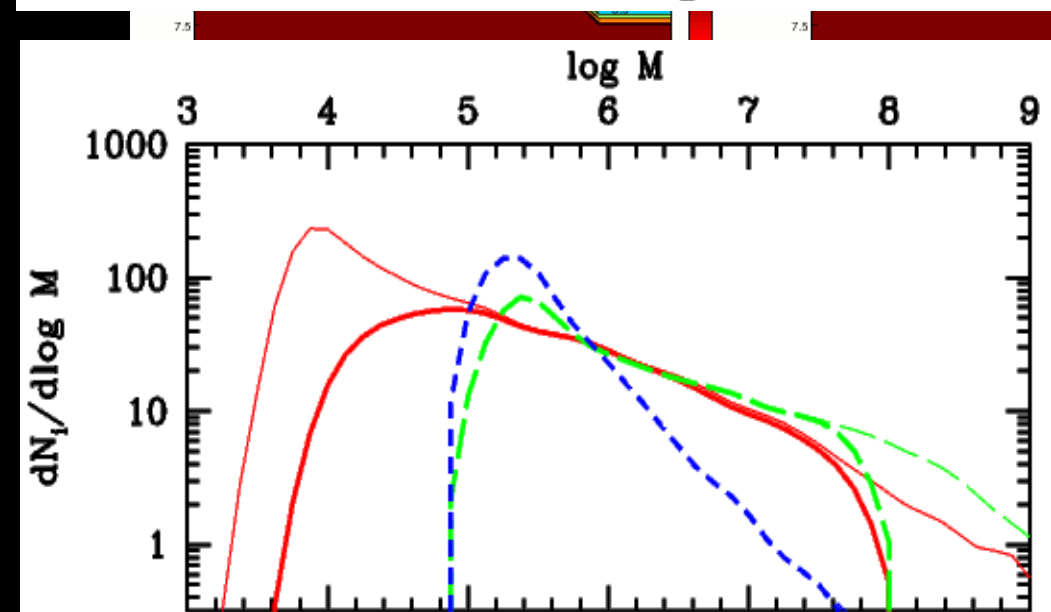
We consider **the distribution $d^3N/dMdqdz$** , we ignore spins.
We use 2PN circular binary waveforms+merger+ringdown
(**PhenomC surrogate**)

1-Construct a detection transfer function



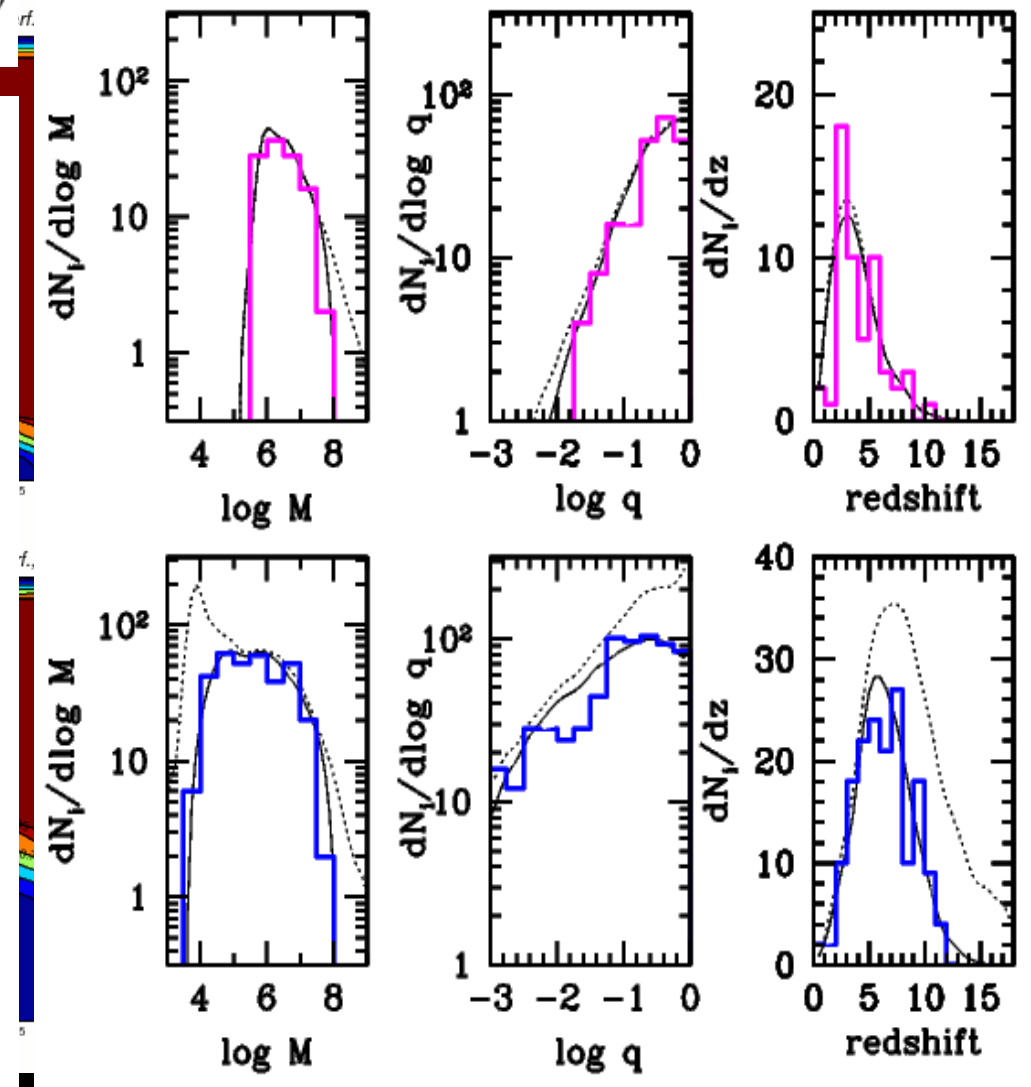
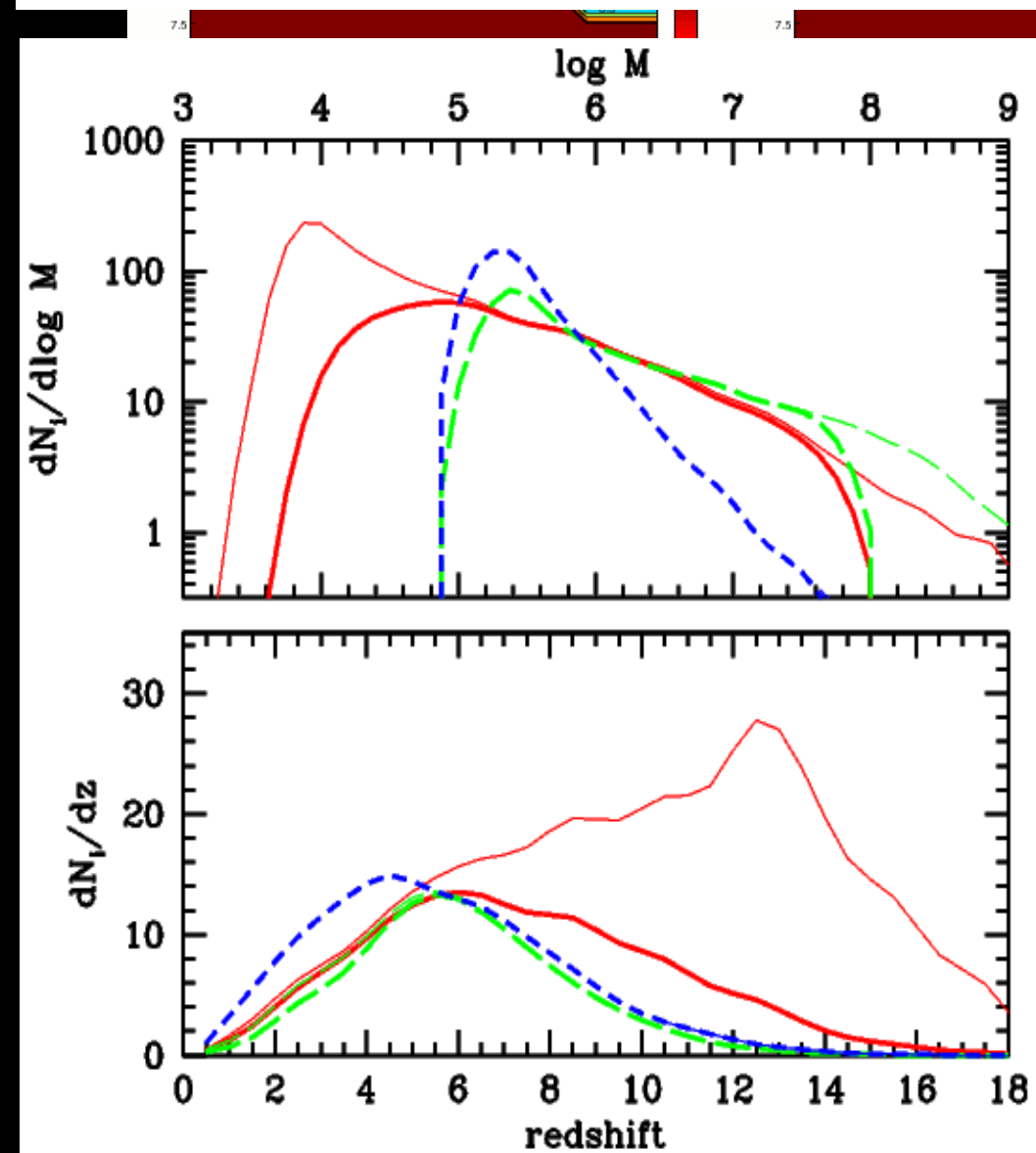
2-Filter the predicted theoretical distribution with the transfer function

$$N_{T_{i,j}}(z, M, q) = \frac{d^3 N_i}{dz dM dq} \times T_j(z, M, q)$$



3-Perform Montecarlo realization of the MBHB population

$$N_{T_{i,j}}(z, M, q) = \frac{d^3 N_i}{dz dM dq} \times T_j(z, M, q)$$



4-Compare observations with theoretical models

Likelihood of the dataset for a given choice of the parameters

$$p(D|\vec{\lambda}, M) = \prod_{i=1}^K \frac{(r_i(\vec{\lambda}))^{n_i} e^{-r_i(\vec{\lambda})}}{n_i!}$$

PURE MODEL COMPARISON: compute the odds ratio

$$O_{AB} = \frac{p(D|A) P(A)}{p(D|B) P(B)}$$

We assign confidence

$p_A = p(D|A)/(p(D|A)+p(D|B))$ to model A

$p_B = 1 - p_A$ to model B

We build probability CDF over 1000 MC realization of the observed population

MIXED MODELS: find the maximum of the posterior

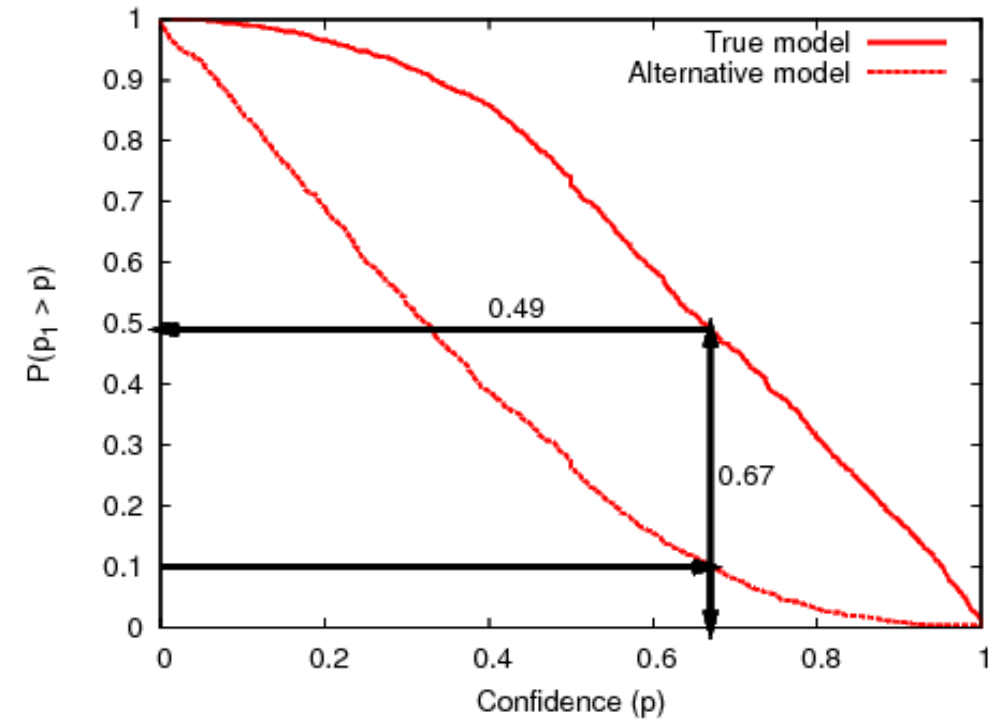
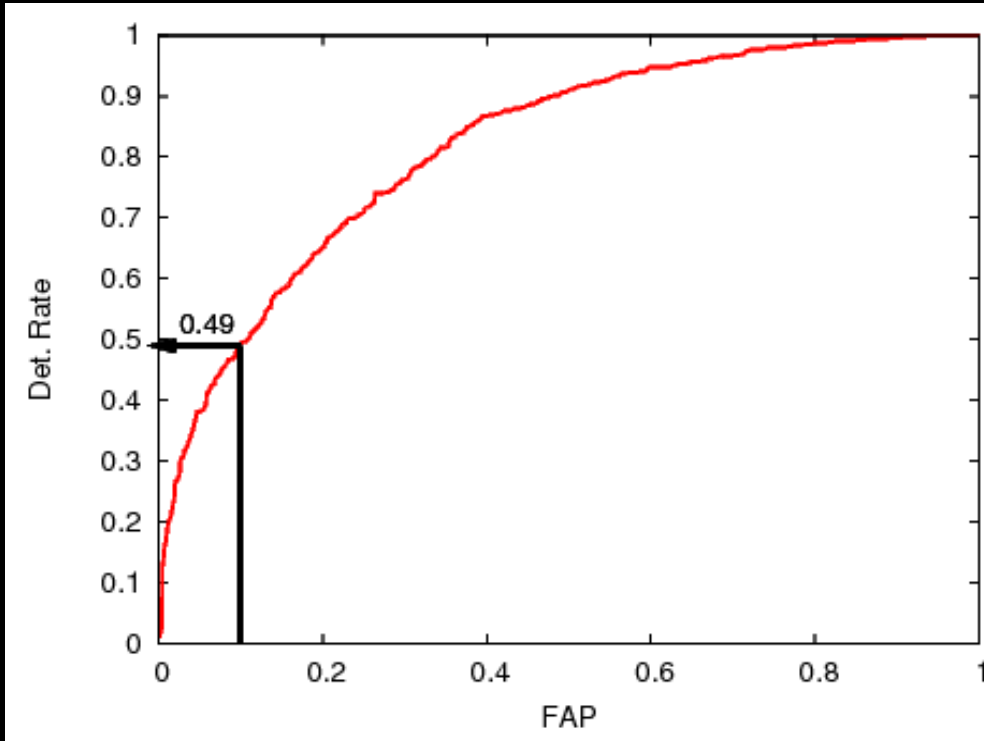
$$p(\vec{\lambda}|D, M) = \frac{p(D|\vec{\lambda}, M) \pi(\vec{\lambda})}{\mathcal{Z}},$$
$$\mathcal{Z} = \int p(D|\vec{\lambda}, M) \pi(\vec{\lambda}) d^N \lambda$$

ROC curves

Pure models:

vs

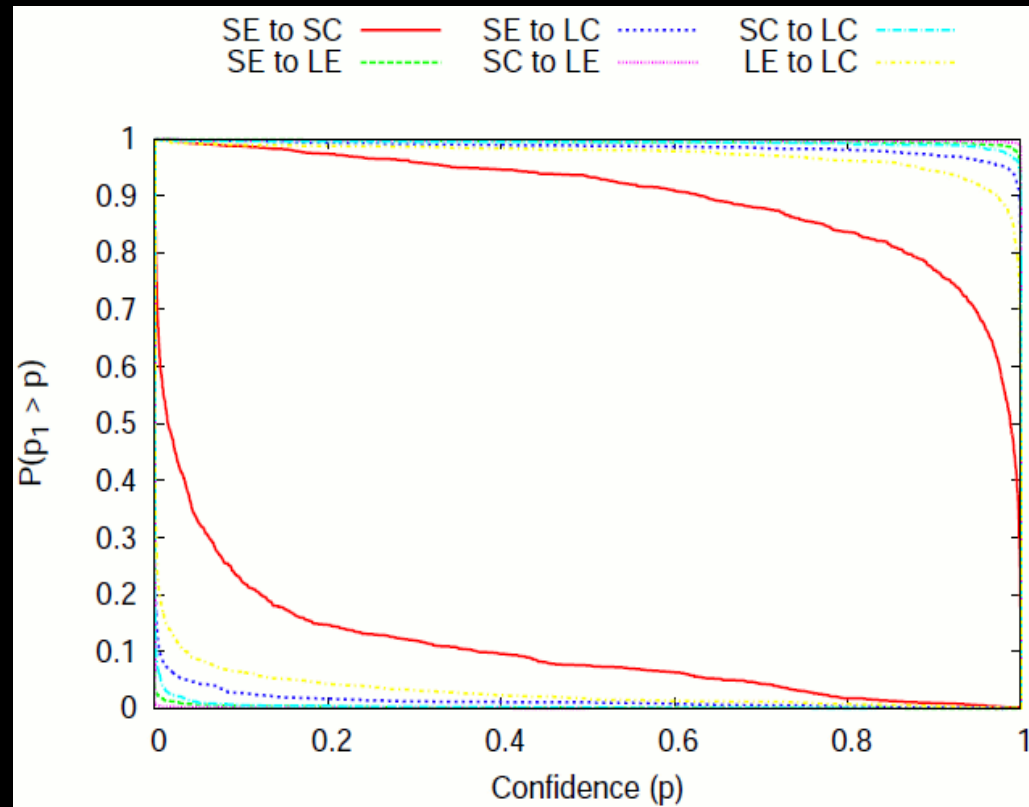
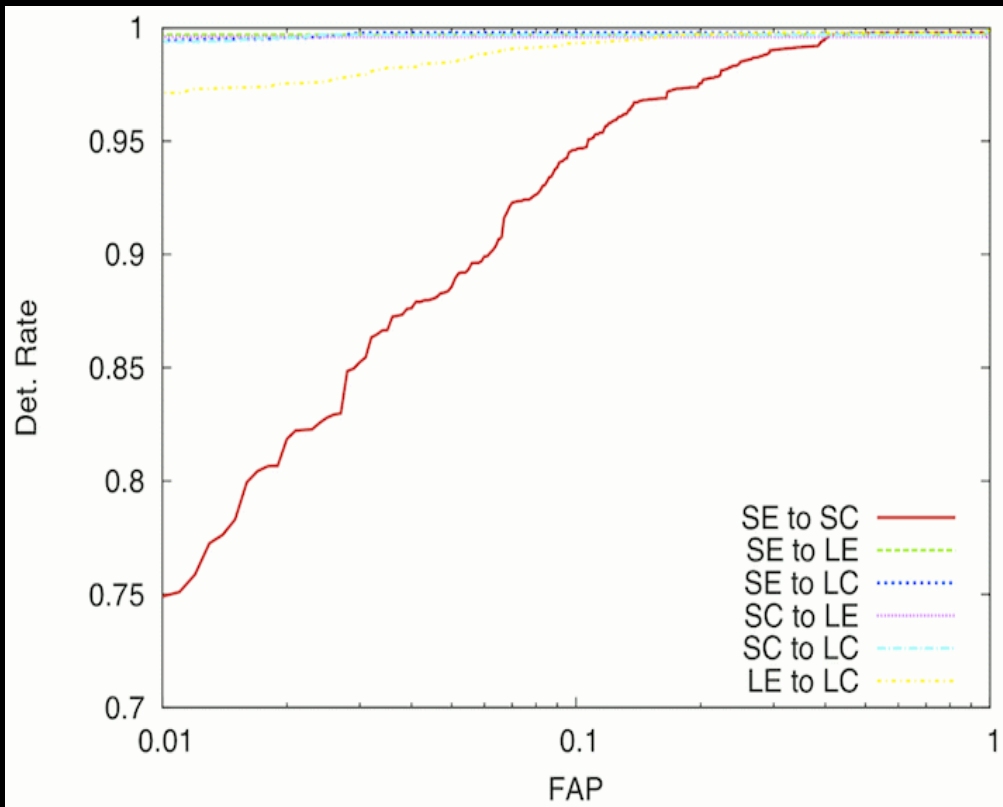
Cumulative distribution function for the confidence



- Take model A(T) and model B(F)
 - Select a threshold in the likelihood ratio
 - The detection rate is the probability that a realization of model A exceeds the threshold
 - The false alarm probability is the frequency with which realization of model B exceed the threshold (false positive)
- MISSING INFO ON THE CONFIDENCE**

- Take the cumulative distribution function of the confidence in A (upper curve)
 - Take the cumulative distribution function of the confidence in B (lower curve)
- RETAINS ALL THE RELEVANT INFO**

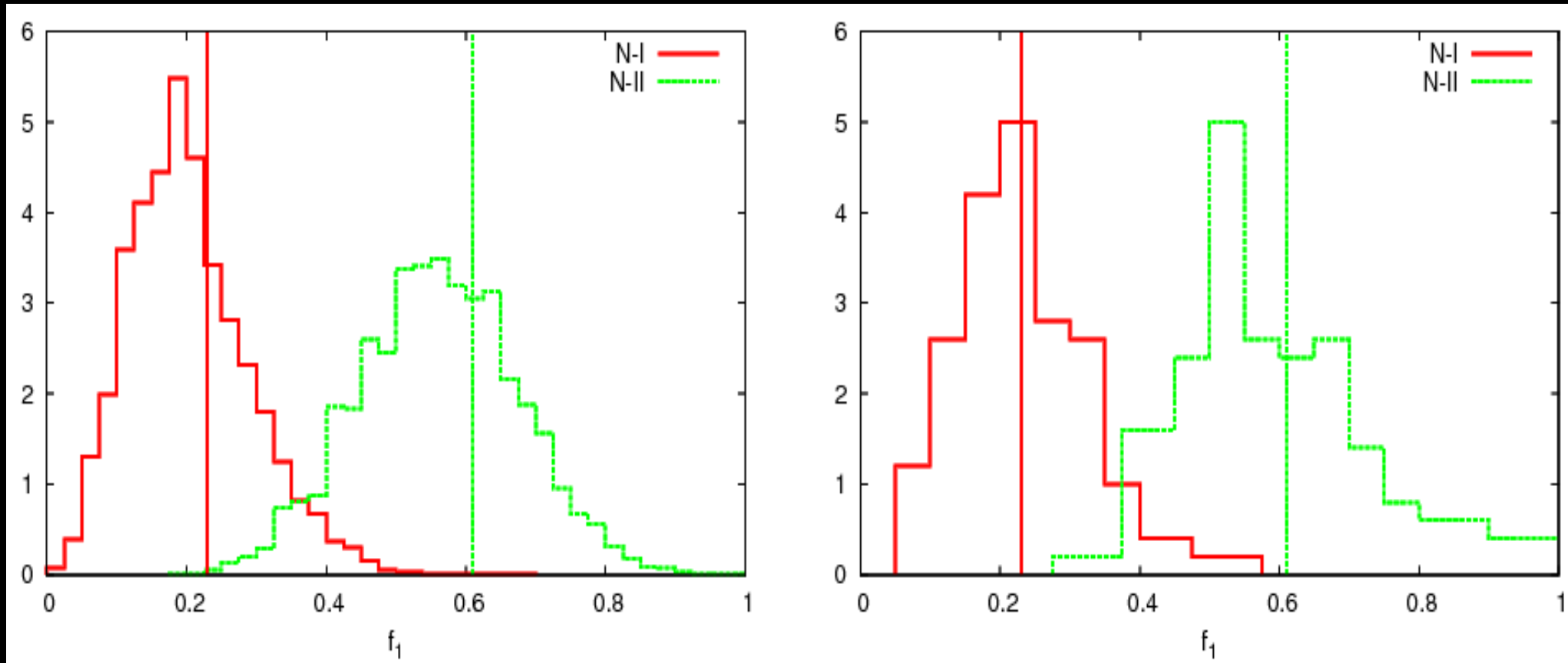
Results



	Without spins				With spins				
	SE	SC	LE	LC	SE	SC	LE	LC	
SE	×	0.48	0.99	0.99	SE	×	0.96	0.99	0.99
SC	0.53	×	1.00	1.00	SC	0.13	×	1.00	1.00
LE	0.01	0.01	×	0.79	LE	0.01	0.01	×	0.97
LC	0.02	0.02	0.22	×	LC	0.02	0.02	0.06	×

**All models are almost perfectly distinguishable
(especially if including spin information)**

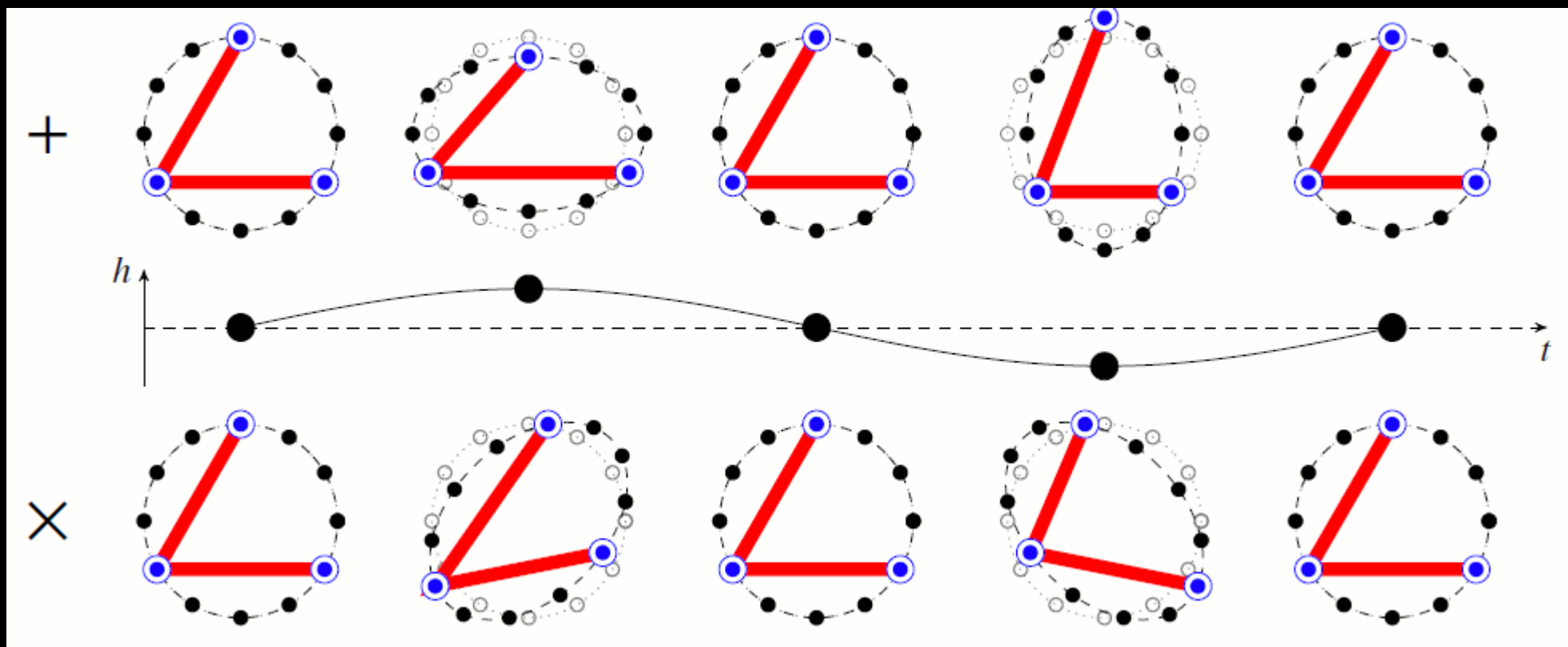
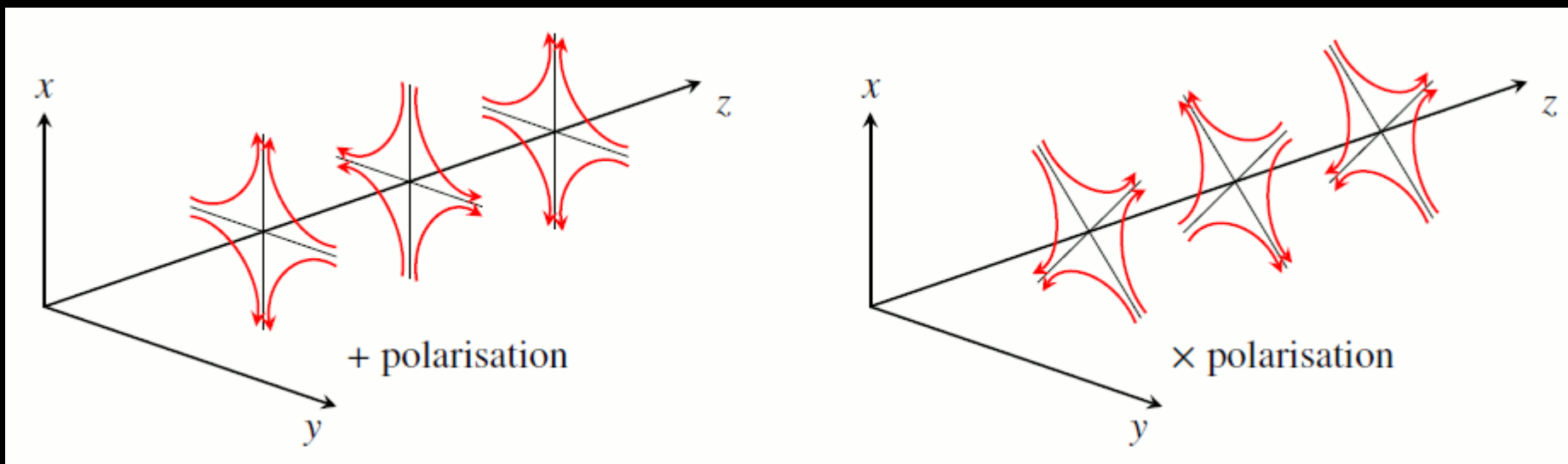
Mixed models: evaluation of the posterior probability distribution function



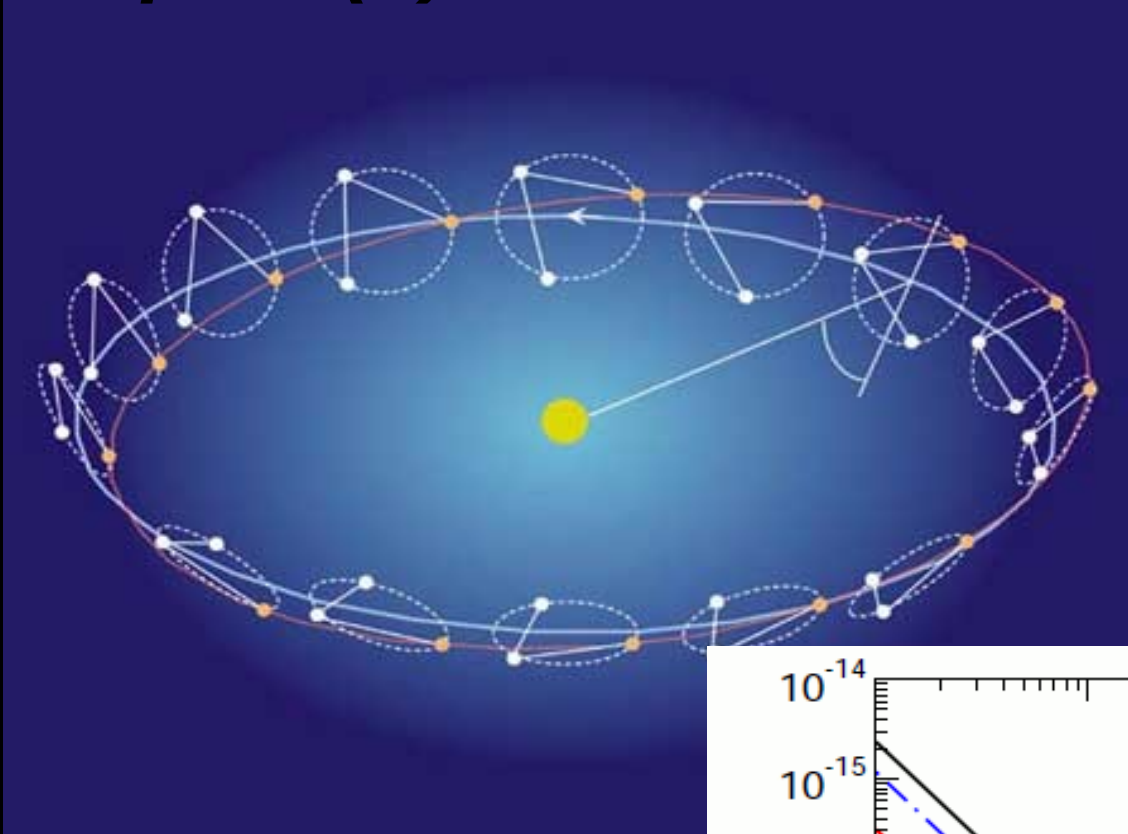
We pin-down the right mixing parameter within 0.1 accuracy!

Summary

- 1- We can detect GWs from compact objects. The GW Encodes all the properties of the source.**
- 2- Analytic techniques and numerical relativity are now producing faithful waveform templates**
- 3- eLISA can detect MBHB GW signals and extract source parameters with unprecedented accuracy ($M < 1\%$ $a < 0.1$ $D_L < 10\%$), but poor sky location.**
- 4- eLISA will detect $\sim < 100$ MBHBs to $z \sim 15$**
- 5- eLISA will provide insights about the early cosmic growth of MBHs impossible to get by any other means.**



European(?) Laser Interferometer Space Antenna



eLISA is sensitive at mHz frequency, where the evolution of MBHBs is fast.

eLISA will detect individual binary inspirals!

eLISA

- same orbit as *LISA*
- 1Gm armlength
- four laser links
- 2 year lifetime
- launch <2022

